

Spin Fluctuation Theory for Quantum Tricritical Point Arising in Proximity to First-Order Phase Transitions: Applications to Heavy-Fermion Systems, YbRh_2Si_2 , CeRu_2Si_2 , and $\beta\text{-YbAlB}_4$

Takahiro MISAWA^{1,2*}, Youhei YAMAJI¹ and Masatoshi IMADA^{1,2}

¹*Department of Applied Physics, University of Tokyo, 7-3-1 Hongo, Bunkyo-ku, Tokyo, 113-8656*

²*JST, CREST, Hongo, Bunkyo-ku, Tokyo 113-8656*

(Received October 29, 2018)

We propose a phenomenological spin fluctuation theory for antiferromagnetic quantum tricritical point (QTCP), where the first-order phase transition changes into the continuous one at zero temperature. Under magnetic fields, ferromagnetic quantum critical fluctuations develop around the antiferromagnetic QTCP in addition to antiferromagnetic ones, which is in sharp contrast with the conventional antiferromagnetic quantum critical point. For itinerant electron systems, we show that the temperature dependence of critical magnetic fluctuations around the QTCP are given as $\chi_Q \propto T^{-3/2}$ ($\chi_0 \propto T^{-3/4}$) at the antiferromagnetic ordering (ferromagnetic) wave number $q = Q$ ($q = 0$). The convex temperature dependence of χ_0^{-1} is the characteristic feature of the QTCP, which is never seen in the conventional spin fluctuation theory. We propose that the general theory of quantum tricriticality that has nothing to do with the specific Kondo physics itself, solves puzzles of quantum criticalities widely observed in heavy-fermion systems such as YbRh_2Si_2 , CeRu_2Si_2 , and $\beta\text{-YbAlB}_4$. For YbRh_2Si_2 , our theory successfully reproduces quantitative behaviors of the experimental ferromagnetic susceptibility and the magnetization curve by choosing the phenomenological parameters properly. The quantum tricriticality is also consistent with singularities of other physical properties such as specific heat, nuclear magnetic relaxation time $1/T_1T$, and Hall coefficient. For CeRu_2Si_2 and $\beta\text{-YbAlB}_4$, we point out that the quantum tricriticality is a possible origin of the anomalous diverging enhancement of the uniform susceptibility observed in these materials.

KEYWORDS: quantum critical phenomena, self-consistent renormalization theory, tricritical point, quantum tricritical point, heavy-fermion systems, YbRh_2Si_2 , CeRu_2Si_2 , $\beta\text{-YbAlB}_4$

1. Introduction

In strongly correlated electron systems, energy scales of interactions among electrons become comparable to those of band widths. Due to such strong correlations, it is often observed that several phases (for instance, normal metals, magnetically ordered phase, and superconducting phase) compete each other. As a consequence of this competition combined with quantum fluctuations, critical temperatures of phase transitions often become zero and a quantum critical point (QCP) emerges.¹⁻³

Heavy-fermion materials are suitable systems for the study of the QCP. In heavy-fermion systems, because of the competition between two energy scales,⁴ namely, the Kondo temperature and the Ruderman-Kittel-Kasuya-Yosida interaction, critical temperatures of magnetic order often become zero and the QCP appears. Actually, QCP has widely been observed in heavy-fermion materials by controlling pressures, external magnetic fields, and chemical substitutions.¹⁻³

Near the QCP, it has been proposed that quantum fluctuations modify the electronic properties drastically. More concretely, electrons do not follow the fundamental and textbook properties of Landau's Fermi liquid, which are universally seen in normal metals. This unconventional behavior is called non-Fermi-liquid behavior.¹⁻³ The non-Fermi-liquid properties of metals have attracted much interest because novel quantum phases

including exotic superconductors are found in the region where such non-Fermi-liquid behaviors are observed.

Around thirty years ago, one of the standard picture to understand the non-Fermi-liquid properties was established,⁵ where non-Fermi-liquid properties have been successfully explained in various cases by spin fluctuations around the QCP of the ordinary second-order transition in the framework of Ginzburg, Landau and Wilson.¹⁻³ We call this standard theory *conventional spin fluctuation theory* which covers so-called self-consistent renormalization (SCR) theory^{6,7} and renormalization-group treatment.^{5,8} In Sec. 2, we will review how the conventional SCR theory describes the non-Fermi liquid behaviors near the QCP.

However, it has been pointed out that this standard picture does not explain recent many experimental results. Even when the apparent QCP is seen, physical properties do not follow the prediction of scalings by the conventional spin fluctuation theory;¹⁻³ i.e., critical exponents of thermodynamic and transport properties do not follow the standard theory, whereas in other cases the critical region is unexpectedly wide. In a number of compounds, this breakdown of the standard theory has been suggested in connection with the proximity of the first-order transition and the effects of inhomogeneities. For example, in weak itinerant ferromagnets ZrZn_2 ,⁹ it has been proposed that the non-Fermi-liquid behavior is robust in a wide range of pressure. Similar behaviors

*E-mail:misawa@solis.t.u-tokyo.ac.jp

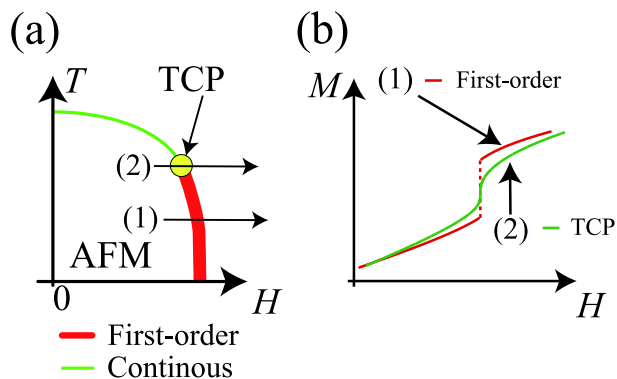


Fig. 1. (Color online) (a) Phase diagram with TCP under magnetic fields. Continuous [First-order] phase transition line is represented by thin (green) [thick (red)] curve, and the TCP is represented by (yellow) circle. (b) Magnetization as a function of magnetic fields near the TCP. (1) At the first-order phase transition, magnetization changes discontinuously. (2) At the TCP, magnetization changes non-analytically and its slope (FM susceptibility $\chi_0 = \partial M / \partial H$) diverges.

are observed in MnSi^{10} and NiS_2 .¹¹ Furthermore, near the first-order transition, a novel quantum phase (nematic fluid) is found in $\text{Sr}_3\text{Ru}_2\text{O}_7$ ¹² and unconventional superconductivity is found in UGe_2 .¹³ When continuous transition switches over to the first-order transition or phase separations, a tricritical point necessarily emerges as the boundary of these two. The purpose of this paper is certainly related to this motivation for elucidating physics under the proximity of first-order transitions and phase separations with the interplay with quantum fluctuations.

A heavy-fermion compound YbRh_2Si_2 is a prototypical example which does not follow the standard theory. It has been proposed that a diverging enhancement of uniform susceptibility χ_0 occurs near the antiferromagnetic (AFM) QCP.¹⁴ The singularity of χ_0 is estimated as $\chi_0 \propto T^{-\zeta}$ with $\zeta \sim 0.6$. Similar diverging enhancements of the uniform susceptibility are observed in CeRu_2Si_2 ¹⁵ ($\chi_0 \propto T^{-\zeta}$ with $\zeta \sim 0.5$) and in $\beta\text{-YbAlB}_4$ ¹⁶ ($\chi_0 \propto T^{-\zeta}$ with $\zeta \sim 0.3$). One might speculate that this diverging enhancement could be caused by the hidden ferromagnetic (FM) QCP coexisting with the observed AFM QCP. However, the criticalities of these diverging uniform susceptibilities can not be explained by the conventional theory, because the critical exponent ζ must always be larger than one for the conventional FM QCP (see Table I).

In our point of view, proximity to the first-order phase transitions is a key to understand the nature of these puzzling quantum criticalities. Actually, in YbRh_2Si_2 and CeRu_2Si_2 , evidences of the first-order AFM phase transitions under magnetic fields are found^{17,18} by tuning the pressure or substituting the chemical elements. In YbRh_2Si_2 , at 2.3 GPa, it has been reported that resistivity changes discontinuously as a function of the magnetic field at low temperatures ($T < 0.5$ K), while it changes continuously at high temperatures ($T > 0.7$ K)¹⁷ as shown in Fig. 2. This indicates that the first-order transition at low temperatures changes into the continuous

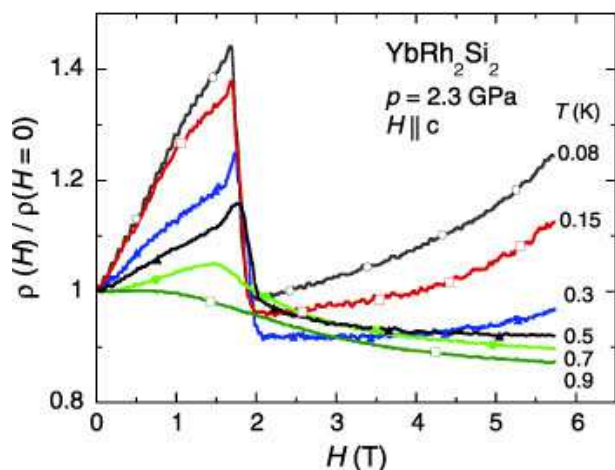


Fig. 2. (Color online) Magnetoresistance $\rho(H)$ of YbRh_2Si_2 at 2.3 GPa reported in Ref. [17]. Discontinuous change of $\rho(H)$ at low temperatures is the evidence of the first-order antiferromagnetic transition.

one at higher temperatures through the tricritical point (TCP), as shown in Fig. 1 (a). In CeRu_2Si_2 , although no clear magnetic order has been found in the stoichiometric compound, AFM order appears in the Rh-substituted material $\text{Ce}(\text{Ru}_{1-x}\text{Rh}_x)_2\text{Si}_2$ for $x > 0.03$. By applying the magnetic fields, it has been observed that the first-order AFM transitions occur at low temperatures in $\text{Ce}(\text{Ru}_{0.9}\text{Rh}_{0.1})_2\text{Si}_2$, while at high temperatures continuous AFM transitions occur.¹⁸ This experimental result indicates that the TCP also exists in $\text{Ce}(\text{Ru}_{1-x}\text{Rh}_x)_2\text{Si}_2$.

In general, tricriticality necessarily induces an additional divergence of uniform fluctuations conjugate to the external field of the control parameter that drives the phase transitions. For example, under magnetic fields, the uniform susceptibility diverges at the AFM TCP.

Here, we intuitively explain why the FM susceptibility diverges at the AFM TCP under magnetic fields. As shown in Fig. 1(b), magnetization jumps at the first-order transition. By approaching the TCP, this jump becomes smaller and vanishes at the TCP. Then, magnetization changes continuously but non-analytically at the TCP. This is the reason why the slope of the magnetization curve, namely, FM susceptibility diverges at the TCP. More precise discussions based on the φ^6 theory are given in Refs. [19, 20].

We note that the criticality of the classical TCP itself does *not* explain the unconventional quantum criticality observed in YbRh_2Si_2 , CeRu_2Si_2 , and $\beta\text{-YbAlB}_4$, because the phase transitions are always either continuous or even absent, namely apparent phase transitions are not observed at ambient pressure and zero magnetic field. By taking YbRh_2Si_2 for example, we propose that the proximity effect of the *quantum tricritical point* (QTCP) is the possible origin of these unconventional quantum criticality. In YbRh_2Si_2 , the first-order phase transition exists at high pressure,¹⁷ while the phase transition is always continuous at ambient pressure. From these experimental results, by decreasing the pressure, we expect that the critical temperature of the TCP becomes zero and the QTCP appears at the critical pressure P_t [see

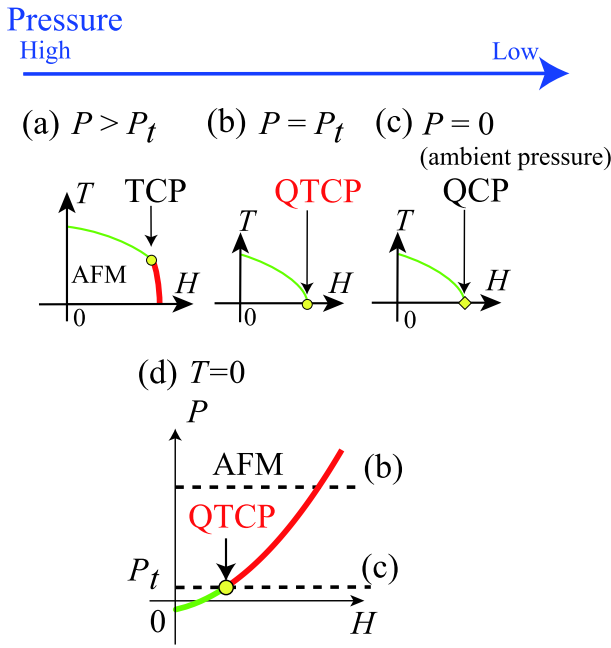


Fig. 3. (Color online)(a)-(c) Expected phase diagrams of YbRh_2Si_2 at various pressures. By decreasing pressure, it is expected that the critical temperatures of the TCP become zero and the QTCP emerges at the critical pressure P_t . (a) Phase diagram with the TCP [(yellow) circle] in T - H plane, where T (H) represents temperature (magnetic field). The TCP separates the continuous [thin (green) curve] and first-order [thick (red) curve] transition lines. In YbRh_2Si_2 , similar phase diagram is proposed at 2.3GPa¹⁷ (see text). (b) Phase diagram with the QTCP. (c) Phase diagram of AFM phase with critical line [solid (green) curve] ending at the QCP [(yellow) diamond]. (d) Phase diagram at zero temperature in P - H plane, where P represents pressure. The QTCP exists between the continuous and first-order transition lines.

Fig. 3(b)]. Because the QTCP is located very close to the ambient pressure, quantum tricriticality can be observed even at ambient pressure where the phase transitions are continuous. The criticality of the QTCP will be clarified in Sec. 3. In Sec. 4.1, we will show that the quantum tricriticality, which induces the divergence of uniform magnetic susceptibility, explains the unconventional quantum criticality observed in YbRh_2Si_2 . In Sec. 4.2 and 4.3, we will discuss that the proximity effect of the QTCP also explains the unconventional quantum criticalities observed in CeRu_2Si_2 and $\beta\text{-YbAlB}_4$.

In this paper, we have clarified the criticality of the QTCP by extending the conventional spin fluctuation theory. In the conventional spin fluctuation theory, the origin of the non-Fermi liquid is ascribed to the coupling of the quasiparticle to the bosonic low-energy fluctuations of the order parameter. However, in the present quantum tricritical case, the quasiparticle couples not only to the bosonic order-parameter fluctuations but also to the uniform mode. Starting with this intuitive picture, we have shown that the serious modification of quantum critical phenomena arises from the equal and combined contribution of the two fluctuations which does not exist in the conventional spin fluctuation theory. We note that the present spin fluctuation theory for the QTCP is applicable to the paramagnetic phase.

A part of the spin fluctuation theory for the QTCP has already been briefly given in Ref. [21]. In this paper, we present the results of the quantum tricriticality in greater detail and discuss the singularities of the physical properties near the QTCP, such as the uniform susceptibility χ_0 , the magnetization M , the specific heat γ , the nuclear relaxation time $1/T_1T$, and the Hall coefficient R_H . We also give thorough comparisons with the experimental results.

Before closing the Introduction, we briefly mention recent theory for the FM QTCP. The FM QTCP has been studied for itinerant helical ferromagnet MnSi ²² by using the renormalization group theory. For nearly FM metal $\text{Sr}_3\text{Ru}_2\text{O}_7$,²³ Green *et al.* have studied the QTCP by extending the SCR theory. However, we note that the singularity of χ_Q^{-1} given by Green *et al.*²³ as $T^{8/3}$ is not correct, since they neglect the T^2 dependence of the bare second-order coefficient r_q ⁸ in their formalism. Moreover, these previous studies on the FM QTCP do not explain the unconventional coexistence of the FM and AFM fluctuations observed in YbRh_2Si_2 .²⁴

The organization of this paper is as follows: In Sec. 2, we briefly review the conventional SCR theory. We mainly explain how the non-Fermi liquid behaviors appear in the conventional SCR theory. In Sec. 3, we present the phenomenological SCR theory for the QTCP. From the present theory, we clarify the criticality of the QTCP; i.e., we obtain the critical exponents of the AFM susceptibility χ_Q , the FM susceptibility χ_0 , and the magnetization curve. Section 4 describes comparisons of the present phenomenological SCR theory with the experimental results of YbRh_2Si_2 , CeRu_2Si_2 , and $\beta\text{-YbAlB}_4$. Section 5 is devoted to a summary and discussion.

2. Conventional spin fluctuation theory for quantum critical point

In this section, to make clear our starting point of the present study, we briefly review the conventional spin fluctuation theory for the quantum critical phenomena. The SCR theory proposed by Moriya is one of the standard theory to describe the quantum critical phenomena. Originally, the SCR theory was proposed to explain the weak and nearly FM or AFM metals.²⁵⁻²⁷ Afterwards, Moriya and Takimoto showed that the SCR theory can be applied to the quantum critical phenomena,^{7,28} namely, they clarified how the spin fluctuations cause the non-Fermi liquid behaviors. We sketch the essence of the phenomenological SCR theory by following Refs. [6, 7, 28].

To understand the essence of the SCR theory, we start from a conventional Ginzburg-Landau-Wilson action for bosonic spin field φ_q at the wave number q :

$$S[\varphi_q] = \frac{1}{2} \sum_q r_q |\varphi_q|^2 + \frac{u}{N_0} \sum_{q, q', q''} (\varphi_q \cdot \varphi_{-q'}) \times (\varphi_{q''} \cdot \varphi_{q'-q-q''}), \quad (1)$$

where u is a constant (we neglect the q dependence of the fourth coefficient u) and N_0 is number of atoms. By

using this action, we obtain the free energy F as

$$\exp(-F/T) = \int \prod_q \mathcal{D}\varphi_q \exp(-S[\varphi_q]/T). \quad (2)$$

Because the contributions from the ordering wave number Q are dominant for the conventional symmetry-breaking phase transitions, we approximate this free energy as a function of AFM order parameter $M^\dagger = \langle \varphi_Q \rangle$ up to the fourth order:

$$F \simeq F_0 = \frac{\tilde{r}_Q}{2} M^{\dagger 2} + u_Q M^{\dagger 4} + \dots, \quad (3)$$

where \tilde{r}_Q is defined as $\tilde{r}_Q = r_Q + 12u_Q\mathcal{K}$, and spin fluctuation term \mathcal{K} is defined as

$$\mathcal{K} = \frac{1}{N_0} \sum_{q \neq Q} \langle |\varphi_q|^2 \rangle. \quad (4)$$

Here, we note that the bare second-order coefficient r_q is renormalized by the spin fluctuation term \mathcal{K} . As we will show later, this spin fluctuation term induces the non-trivial temperature dependence of the physical properties near the QCP. Hereafter, we only consider the paramagnetic state, i.e., $M^\dagger = 0$.

By using the free energy in eq. (3), we obtain the ordering susceptibility χ_Q as

$$\chi_Q^{-1} = \left. \frac{\partial^2 F_0}{\partial M^{\dagger 2}} \right|_{M^\dagger \rightarrow 0} = \tilde{r}_Q = r_Q + 12u_Q\mathcal{K}. \quad (5)$$

According to the fluctuation-dissipation theorem,²⁹ the spin fluctuation term \mathcal{K} is described as

$$\begin{aligned} \mathcal{K} &= \frac{1}{N_0} \sum_{q \neq Q} \langle |\varphi_q|^2 \rangle \\ &= \frac{2}{\pi N_0} \int_0^\infty d\omega \left(\frac{1}{2} + n(\omega) \right) \sum_{q \neq Q} \text{Im} \chi(q, \omega), \end{aligned} \quad (6)$$

where $n(\omega) \equiv 1/(e^{\omega/T} - 1)$. Near the QCP, we assume that $\chi(Q + q, \omega)$ can be expanded with respect to q and ω as follows:

$$\chi^{-1}(Q + q, \omega) \sim \chi_Q^{-1} + Aq^2 - i \frac{C\omega}{q^\theta}, \quad (7)$$

where $\theta = 1[\theta = 0]$ for the FM transitions ($Q = 0$) [AFM transitions ($Q \neq 0$)]. Here A and C are constants.

From eqs. (6) and (7), \mathcal{K} is described as

$$\begin{aligned} \mathcal{K} &= \frac{2K_d v_0}{\pi} \int_0^{q_c} dq \int_0^\infty d\omega \left(\frac{1}{2} + n(\omega) \right) \\ &\quad \times \frac{C\omega q^{d+\theta-1}}{[q^\theta(\chi_Q^{-1} + Aq^2)]^2 + (C\omega)^2} \\ &= \frac{K_d v_0}{\pi} \int_0^{q_c} dq \int_0^\infty d\omega \frac{C\omega q^{d+\theta-1}}{[q^\theta(\chi_Q^{-1} + Aq^2)]^2 + (C\omega)^2} \\ &\quad + \frac{2K_d v_0}{\pi} \int_0^{q_c} dq \int_0^\infty d\omega \frac{Cn(\omega)\omega q^{d+\theta-1}}{[q^\theta(\chi_Q^{-1} + Aq^2)]^2 + (C\omega)^2} \\ &= \mathcal{K}(0) + \mathcal{K}(T), \end{aligned} \quad (8)$$

where d (T) represents the spatial dimensions (temperatures) and v_0 is the volume of the unit cell; K_d is defined

as $K_d = S_d/(2\pi)^d$, where $S_d = 2\pi^{d/2}/\Gamma(d/2)$ and Γ is the gamma function; q_c is the cutoff wave number. Equations (5) and (8) constitute the self-consistent equation to be solved.

For the brief notation, we introduce the variables as

$$\begin{aligned} q_B &= (2d\pi^{d-1}/v_0)^{\frac{1}{d}}, & x &= q/q_B, \\ T_A &= \frac{Aq_B^2}{2}, & T_0 &= \frac{Aq_B^{2+\theta}}{2\pi C}, \\ z &= \frac{\omega}{2\pi T}, & z' &= \frac{\omega}{2\pi}, \\ y &= \frac{\chi(Q)^{-1}}{2T_A}, & t &= \frac{T}{T_0}. \end{aligned}$$

Here, we note that the parameter T_A and T_0 are so-called SCR parameters. Typical values of them in real materials are given in Refs. [6, 7]. By using these variables, we can describe $\mathcal{K}(0)$ and $\mathcal{K}(T)$ as

$$\begin{aligned} \mathcal{K}(0) &= \frac{T_0 d}{T_A} \int_0^\infty dz' \int_0^{x_c} \frac{x^{d+\theta-1} dx}{[(y+x^2)x^\theta]^2 + z'^2}, \quad (9) \\ \mathcal{K}(T) &= \frac{2T_0 d}{T_A} \int_0^\infty \frac{z dz}{e^{2\pi z} - 1} \int_0^{x_c} \frac{x^{d+\theta-1} dx}{[(y+x^2)x^\theta/t]^2 + z^2}. \end{aligned} \quad (10)$$

Then, we obtain the singularity of $\mathcal{K}(0)$ and $\mathcal{K}(T)$. In three dimensions, because $\mathcal{K}(0)$ can be expanded with respect to y regularly, we obtain the relation as

$$\mathcal{K}(0) = K_0 - K_1 y. \quad (11)$$

Temperature dependence of $\mathcal{K}(T)$ is obtained by the simple scaling argument. To see the temperature dependence of $\mathcal{K}(T)$ directly, we introduce the variable x' as $x = x' t^{1/2+\theta}$. By using this relation, we obtain

$$\mathcal{K}(T) = t^{\frac{d+\theta}{2+\theta}} I(t), \quad (12)$$

$$I(t) = \frac{2T_0 d}{T_A} \int_0^\infty \frac{z dz}{e^{2\pi z} - 1} \int_0^{x'_c} \frac{x' dx'^{d+\theta-1}}{[(y/t^{\frac{2+\theta}{2+\theta}} + x'^2)x'^\theta]^2 + z^2}. \quad (13)$$

In three dimensions, $I(t)$ converges to a constant at zero temperature ($t \rightarrow 0$) if the condition

$$\lim_{t \rightarrow \infty} y/t^{2/2+\theta} \rightarrow 0$$

is satisfied.

In contrast to three dimensions, in two dimensions, $I(t)$ has a logarithmic divergence and the analysis becomes complicated. We do not show the complete analysis here, because it is not the essential part of the SCR theory. To know the details of calculations for the two dimensional case, see Refs. [6, 28]. Hereafter, we mainly consider the three dimensional case.

From eqs. (5), (11), and (13), we obtain the relation

$$y = y_0 + 12u_Q(K_0 - K_1 y + t^{\frac{d+\theta}{2+\theta}} I(t)), \quad (14)$$

where $y_0 = r_Q/2T_A$. This relation leads to

$$y = \tilde{y}_0 + \tilde{y}_1 t^{\frac{d+\theta}{2+\theta}}, \quad (15)$$

where $\tilde{y}_0 = (y_0 + 12u_Q K_0)/(1 + 12u_Q K_1)$ and $\tilde{y}_1 = I(t)/(1 + 12u_Q K_1)$. The location of the QCP is given

Physical Properties	3D AFM	3D FM	2D AFM	2D FM
χ_Q^{-1}	$T^{3/2}$	$T^{4/3}$	$-T \log \log T / \log T$	$-\log T$
$\gamma = C/T$	const. $- T^{1/2}$	$-\log T$	$-\log T$	$T^{-1/3}$
$1/T_1 T$	$\chi_Q^{1/2}$	χ_0	χ_Q	$\chi_0^{3/2}$
ρ	$T^{3/2}$	$T^{5/3}$	T	$T^{4/3}$

Table I. Critical exponents for the conventional QCP. For the AFM (FM) QCP, the ordering wave number Q is defined as $Q \neq 0$ ($Q = 0$).

by $\tilde{y}_0 = 0$. Therefore, the singularity of the ordering susceptibility near the QCP is obtained as

$$\chi_Q^{-1} \propto T^{3/2} \quad (3\text{D AFM QCP}), \quad (16)$$

$$\chi_0^{-1} \propto T^{4/3} \quad (3\text{D FM QCP}). \quad (17)$$

In two dimensions, by evaluating the singularities of $\mathcal{K}(0)$ and $\mathcal{K}(T)$ carefully, we obtain the singularities of ordering susceptibility as

$$\chi_Q^{-1} \propto -T \log |\log T| / \log T \quad (2\text{D AFM QCP}), \quad (18)$$

$$\chi_0^{-1} \propto -T \log T \quad (2\text{D FM QCP}). \quad (19)$$

By using the singularity of the ordering fluctuation, we can obtain the singularities of the specific heat,³⁰ the nuclear relaxation time $1/T_1 T$,^{31,32} and the electronic resistivity ρ .^{7,33,34} Details of the calculations are shown in Refs. [6,28]. Finally, we summarize the criticalities of the conventional QCP in Table. I.

3. Spin fluctuation theory for quantum tricritical point

To clarify the criticality of the QTCP under magnetic fields, we extend the conventional Ginzburg-Landau-Wilson action in eq. (1), up to the sixth order of the bosonic field φ , as

$$S[\varphi_q] = \frac{1}{2} \sum_q r_q |\varphi_q|^2 + \frac{1}{N_0} \sum_{q,q',q''} u(q,q',q'') (\varphi_q \cdot \varphi_{-q'}) \times (\varphi_{q''} \cdot \varphi_{q'-q-q''}) \quad (20)$$

$$+ \frac{v}{N_0^2} \sum_{q_1 \sim q_5} (\varphi_{q_1} \cdot \varphi_{-q_2}) (\varphi_{q_3} \cdot \varphi_{-q_4}) \times (\varphi_{q_5} \cdot \varphi_{q_2+q_4-q_1-q_3-q_5}) - H \varphi_0, \quad (21)$$

where H (N_0) is an external magnetic field (number of atoms); $u(q, q', q'')$ and v are constants, while r_q depends on the magnetic field H . From eq. (21), the free energy F is obtained from

$$\exp(-F/T) = \int \prod_q \mathcal{D}\varphi_q \exp(-S[\varphi_q]/T). \quad (22)$$

Since the QTCP is expressed by fluctuations at both the AFM Bragg wave number $q = Q$ and zero wave number $q = 0$, we approximate the free energy as a function of the order parameter $M^\dagger = \langle \varphi_Q \rangle$ and the uniform magnetization $M = \langle \varphi_0 \rangle$:

$$F_0 = \frac{1}{2} \tilde{r}_Q M^{\dagger 2} + \tilde{u}_Q M^{\dagger 4} + v M^{\dagger 6} + \frac{1}{2} \tilde{r}_0 M^2 + \tilde{u}_0 M^4 + v M^6 - H M, \quad (23)$$

where \tilde{r}_Q , \tilde{u}_Q , \tilde{r}_0 , \tilde{u}_0 , and \mathcal{K} are defined as

$$\tilde{r}_Q(T, H) = r_Q(H) + 12u_Q(\mathcal{K} + M^2) + 90v(\mathcal{K} + M^2)^2, \quad (24)$$

$$\tilde{u}_Q(T, H) = u_Q + 15v(\mathcal{K} + M^2), \quad (25)$$

$$\tilde{r}_0(T, H) = r_0(H) + 12u_0\mathcal{K} + 90v\mathcal{K}^2, \quad (26)$$

$$\tilde{u}_0(T, H) = u_0 + 15v\mathcal{K}, \quad (27)$$

$$\mathcal{K} = \frac{1}{N_0} \sum_{q \neq 0, Q} \langle |\varphi_q|^2 \rangle. \quad (28)$$

Effects of spin fluctuations are included in \mathcal{K} following the conventional SCR theory. We approximate $u(q, q, Q)$ [$u(q, q, 0)$] and the equivalent coefficients as q -independent values; $u(q, q, Q) \simeq u_Q$ [$u(q, q, 0) \simeq u_0$] for all q [for $q \neq Q$].

We eliminate M in eq. (23) by using the saddle-point condition for M , $\partial F_0 / \partial M = 0$, leading to the following relation between M and M^\dagger as

$$M = a_0 + a_1 M^{\dagger 2} + a_2 M^{\dagger 4} + \dots, \quad (29)$$

where the expansion coefficients a_0 to a_2 are determined by substituting eq. (29) into the saddle-point condition:

$$\tilde{r}_0(T, H)a_0 + 4\tilde{u}_0(T, H)a_0^3 + 6va_0^5 - H = 0, \quad (30)$$

$$12a_0\tilde{u}_Q(T, H) + a_1 R(T, H) = 0, \quad (31)$$

where $R(T, H) = \tilde{r}_0(T, H) + 12\tilde{u}_0(T, H)a_0^2 + 30va_0^4$. By using eq. (29), we obtain the free energy as

$$F_0 = \frac{1}{2} \tilde{r}_Q(T, H) M^{\dagger 2} + \tilde{u}'_Q(T, H) M^{\dagger 4} + O(M^{\dagger 6}), \quad (32)$$

where $\tilde{u}'_Q(T, H) = \tilde{u}_Q(T, H)(1 + 6a_0a_1)$. In eq. (32), continuous phase transitions occur at $\tilde{r}_Q = 0$ when $\tilde{u}'_Q(T, H) > 0$, while the first-order phase transitions occur when $\tilde{u}'_Q(T, H) < 0$.^{19,20} Therefore, the QTCP appears when the conditions $\tilde{r}_Q(0, H_t) = 0$ and $\tilde{u}_Q(0, H_t) = 0$ are both satisfied, where H_t is the critical field at the QTCP.

We now discuss the susceptibilities χ_Q at the AFM ordering vector Q and χ_0 at $q = 0$ in the disordered phase ($M^\dagger = 0$, $M = a_0$) by using eq. (30) and the free energy (32). From eq. (32), χ_Q^{-1} is given as

$$\chi_Q^{-1} = \left. \frac{\partial^2 F_0}{\partial M^{\dagger 2}} \right|_{M^\dagger=0} = \tilde{r}_Q(T, H). \quad (33)$$

By differentiating eq. (30) with respect to the magnetic field H , we obtain χ_0^{-1} as

$$\chi_0^{-1} \equiv \left(\frac{\partial a_0}{\partial H} \right)^{-1} = \frac{R(T, H)}{1 - a_0 \partial \tilde{r}_0 / \partial H - 4a_0^3 \partial \tilde{u}_0 / \partial H} \propto \tilde{u}_Q(T, H). \quad (34)$$

Here, we used eq. (31), which gives $R(T, H) \propto \tilde{u}_Q(T, H)$. Detailed derivation of eq. (34) is given in Appendix [see eq. (A.4)].

Here, we note that $\tilde{r}_Q(T, H)$ and $\tilde{u}_Q(T, H)$ in the right hand sides of eqs. (33) and (34) are expressed by \mathcal{K} by using eqs. (24) and (25). Since \mathcal{K} is given from $\text{Im}\chi$ by the fluctuation-dissipation theorem²⁹ as eq. (6), \mathcal{K} can be expressed by using χ_Q and χ_0 . Therefore, by using eqs. (33) and (34), we can determine the singularities of the susceptibilities (χ_Q and χ_0) self-consistently. Once the singularities of χ_Q and χ_0 are determined, we can determine the singularities of a_0 by using eq. (30). Hereafter, by using the above self-consistent equations, we clarify how the susceptibilities and the magnetization measured from the QTCP ($\chi_Q, \chi_0, \delta a_0 \equiv a_0 - a_{0t}$ with a_{0t} being the value at the QTCP) are scaled with $\delta H = H - H_t$ and T near the QTCP. The results will be shown in eqs. (61)-(63) and Table II.

As we have shown in the last section, in the SCR theory, the nontrivial temperature dependence of physical properties originates from the spin fluctuation term \mathcal{K} . Therefore, we need to clarify the scaling of \mathcal{K} by using the fluctuation-dissipation theorem by combining with expansions of $\chi_{0+q}(\omega)$ and $\chi_{Q+q}(\omega)$ in terms of the wave number q and the frequency ω near the QTCP. The fluctuation-dissipation theorem gives the relation

$$\sum_{q \neq 0, Q} \langle |\varphi_q|^2 \rangle = \frac{2}{\pi} \int_0^\infty d\omega \left(\frac{1}{2} + \frac{1}{e^{\omega/T} - 1} \right) \sum_{q \neq 0, Q} \text{Im}\chi(q, \omega). \quad (35)$$

Hereafter, we mainly consider the three dimensional case.

First, we consider the singularity of \mathcal{K} near the ordering wave number. The ordering susceptibility $\chi_{Q+q}(\omega)$ is assumed to follow the conventional Ornstein-Zernike form,

$$\chi_{Q+q}(\omega)^{-1} \simeq \chi_Q^{-1} + A_Q q^2 - iC_Q \omega, \quad (36)$$

as in the conventional SCR formalism. From eqs. (35) and (36), in three dimensions, we evaluate \mathcal{K} near the ordering wave number as

$$\begin{aligned} \mathcal{K}_Q &= \frac{2}{\pi N_0} \int_0^\infty d\omega \left(\frac{1}{2} + n(\omega) \right) \sum_{q \sim Q} \text{Im}\chi(q, \omega) \\ &= \frac{v_0 K_3}{\pi} \int_0^{q_c} dq \int_0^\infty d\omega \frac{C_Q \omega q^2}{[(\chi_Q^{-1} + A_Q q^2)^2 + (C_Q \omega)^2]} \\ &\quad + \frac{2v_0 K_3}{\pi} \int_0^{q_c} dq \int_0^\infty d\omega \frac{n(\omega) C_Q \omega q^2}{[(\chi_Q^{-1} + A_Q q^2)^2 + (C_Q \omega)^2]} \\ &= \mathcal{K}_Q(0) + \mathcal{K}_Q(T), \end{aligned} \quad (37)$$

where $\mathcal{K}_Q(0)$ is the so-called zero point fluctuations and v_0 is the volume of the unit cell; K_3 is defined as $K_3 = S_3/(2\pi)^3$, where $S_3 = 2\pi^{3/2}/\Gamma(3/2) = 4\pi$. For the brief notation, we introduce the variables as

$$\begin{aligned} q_B &= (6\pi^2/v_0)^{\frac{1}{3}}, & T_{QA} &= \frac{A_Q q_B^2}{2}, \\ T_{Q0} &= \frac{A_Q q_B^2}{2\pi C_Q}, & q &= q_B x, \\ z &= \frac{\omega}{2\pi T}, & z' &= \frac{\omega}{2\pi}, \end{aligned}$$

$$y(Q) = \frac{\chi(Q)^{-1}}{2T_{QA}}, \quad t(Q) = \frac{T}{T_{Q0}}.$$

By using these variables, we obtain

$$\begin{aligned} \mathcal{K}_Q(0) &= \frac{3T_{Q0}}{T_{QA}} \int_0^\infty dz' \int_0^{x_c} \frac{x^2 dx}{(y(Q) + x^2)^2 + z'^2}, \quad (38) \\ \mathcal{K}_Q(T) &= \frac{6T_{Q0}}{T_{QA}} \int_0^\infty \frac{z dz}{e^{2\pi z} - 1} \int_0^{x_c} \frac{x^2 dx}{[(y(Q) + x^2)/t]^2 + z^2} \end{aligned} \quad (39)$$

Here, we examine the temperature dependence of $\mathcal{K}_Q(T)$ and $\mathcal{K}_Q(0)$. By scaling x as $x = t^{1/2} x'$, we obtain the singularity of $\mathcal{K}_Q(T)$ as

$$\mathcal{K}_Q(T) = t^{3/2} I_Q(t) \quad (40)$$

$$I_Q(t) = \frac{6T_{Q0}}{T_{QA}} \int_0^\infty \frac{z dz}{e^{2\pi z} - 1} \int_0^{x'_c} \frac{x'^2 dx'}{(y(Q)/t + x'^2)^2 + z^2}. \quad (41)$$

Because self-consistent equations require the condition $y(Q)/t \ll 1$ for small t , $I_Q(t)$ becomes constant at zero temperature. Therefore, near the QTCP, we obtain the singularity of $\mathcal{K}_Q(T)$ as

$$\mathcal{K}_Q(T) \propto T^{3/2}. \quad (42)$$

Because $\mathcal{K}_Q(0)$ can be expanded with respect to $y(Q)$, we obtain the singularity of $\mathcal{K}_Q(0)$ as

$$\mathcal{K}_Q(0) \simeq K_{Q0} - K_{Q1} \chi_Q^{-1}, \quad (43)$$

where K_{Q0} and K_{Q1} are constants.

Next, we consider the singularity of \mathcal{K} near zero wave number. We note that the enhancement of the uniform susceptibility is not caused by the conventional symmetry-breaking phase transition but is caused by the first-order AFM phase transition. Therefore, in contrast to the ordering susceptibility, the uniform part $\chi_{0+q}(\omega)$ does *not* follow the conventional Ornstein-Zernike form. Actually, according to the Ginzburg-Landau-Wilson theory,¹⁹ the scaling relation $\chi_0^{-1}(0) \propto \chi_Q^{-1/2}(0)$ holds near the TCP. As we will see, the self-consistency among eqs. (28), (30), (33), (34), and (35) requires that this relation still holds for $q \neq 0$. Therefore, we obtain the relation

$$\begin{aligned} \chi_{0+q}(0)^{-1} &\propto \chi_{Q+q}(0)^{-1/2} \\ &\propto (\chi_Q^{-1} + A_Q q^2)^{1/2} \propto (\chi_0^{-2} + A_0 q^2)^{1/2}. \end{aligned} \quad (44)$$

From the conservation law, the ω dependence of $\chi_{0+q}(\omega)^{-1}$ should be given as $\chi_{0+q}(\omega)^{-1} \simeq \chi_{0+q}(0)^{-1} - iC_0 \omega/q$. Finally, we obtain ω and q expansions of $\chi_{0+q}(\omega)^{-1}$ as

$$\chi_{0+q}(\omega)^{-1} \simeq (\chi_0^{-2} + A_0 q^2)^{1/2} - iC_0 \omega/q. \quad (45)$$

From eqs. (35) and (45), we evaluate \mathcal{K} near the zero

wave number as

$$\begin{aligned}\mathcal{K}_0 &= \frac{2}{\pi} \int_0^\infty d\omega \left(\frac{1}{2} + n(\omega) \right) \sum_{q \sim 0} \text{Im} \chi(q, \omega) \\ &= \frac{K_3 v_0}{\pi} \int_0^{q_c} dq \int_0^\infty d\omega \frac{C_0 \omega q^3}{[(\chi_0^{-2} + A_0 q^2)q^2 + (C_0 \omega)]} \\ &+ \frac{2K_3 v_0}{\pi} \int_0^{q_c} dq \int_0^\infty d\omega \frac{n(\omega) C_0 \omega q^3}{[(\chi_0^{-2} + A_0 q^2)q^2 + (C_0 \omega)^2]} \\ &= \mathcal{K}_0(0) + \mathcal{K}_0(T),\end{aligned}\quad (46)$$

For the brief notation, we introduce the variables as

$$\begin{aligned}y(0) &= \frac{\chi(0)^{-1}}{2T_{0A}}, & T_{0A} &= (A_0 q_B^2/4)^{1/2}, \\ t(0) &= \frac{T}{T_{00}}, & T_{00} &= q_B T_{0A}/\pi C_0.\end{aligned}$$

By using these variables, we obtain

$$\begin{aligned}\mathcal{K}_0(0) &= \frac{3T_{00}}{T_{0A}} \int_0^\infty dz' \int_0^{x_c} \frac{x^2 dx}{[y(0)^2 + x^2]x^2 + z'^2}, \quad (47) \\ \mathcal{K}_0(T) &= \frac{6T_{00}}{T_{0A}} \int_0^\infty \frac{z dz}{e^{2\pi z} - 1} \int_0^{x_c} \frac{x^2 dx}{[(y(0)^2 + x^2)/t]x^2 + z^2}.\end{aligned}\quad (48)$$

By scaling x as $x = x't^{1/2}$, we obtain

$$\begin{aligned}\mathcal{K}_0(T) &= t^2 I_0(t) \quad (49) \\ I_0(t) &= \frac{6T_{00}}{T_{0A}} \int_0^\infty \frac{z dz}{e^{2\pi z} - 1} \int_0^{x'_c} \frac{x'^2 dx}{(y(0)^2/t + x'^2)x'^2 + z^2}.\end{aligned}\quad (50)$$

Because $I_0(t)$ becomes constant at zero temperatures, near the QTCP, we obtain the singularity of $\mathcal{K}_0(T)$ as

$$\mathcal{K}_0(T) \propto T^2. \quad (51)$$

Because $\mathcal{K}_0(0)$ can be expanded with respect to $y(0)^2$, we obtain the singularity of $\mathcal{K}_0(0)$ as

$$\mathcal{K}_0(0) \simeq K_{00} - K_{01} \chi_0^{-2}, \quad (52)$$

where K_{00} and K_{01} are constants. From eqs.(42), (43), (51), and (52), we obtain the singularity of $\delta\mathcal{K} = \mathcal{K} - \mathcal{K}_t$ measured from the critical value \mathcal{K}_t as

$$\delta\mathcal{K} \simeq -K_{01} \chi_0^{-2} - K_{Q1} \chi_Q^{-1} + K_{0T} T^2 + K_{QT} T^{3/2}. \quad (53)$$

Now the singularity of magnetization a_0 is obtained by solving eq. (30). Near the QTCP, eq. (30) can be approximated as

$$A \delta a_0^2 + B \delta a_0 + C = 0, \quad (54)$$

with $A = 12a_{0t}(5va_{0t}^2 + \tilde{u}_0)$, $B = \delta\tilde{r}_0 + 12a_{0t}^2 \delta\tilde{u}_0$, and $C = a_{0t} \delta\tilde{r}_0 + 4a_{0t}^3 \delta\tilde{u}_0 - \delta H$, where $\delta\tilde{r}_0 = \tilde{r}_0(T, H) - \tilde{r}_0(0, H_t)$, and $\delta\tilde{u}_0 = \tilde{u}_0(T, H) - \tilde{u}_0(0, H_t)$. Since both B and C vanish at the QTCP, we obtain the asymptotic behavior of δa_0 as

$$\delta a_0 \simeq (\alpha_0 \delta H + \alpha_1 \delta\mathcal{K})^{1/2}, \quad (55)$$

where α_0 and α_1 are constants. We give detailed derivation of eq. (55) in Appendix [see eq. (A.1)].

Physical Properties	T dependence	H dependence
χ_Q	$T^{-3/2}$	δH^{-1}
χ_0	$T^{-3/4}$	$\delta H^{-1/2}$
δM	$T^{3/4}$	$\delta H^{1/2}$

Table II. Critical exponents for QTCP. Here, T and H represent temperature and magnetic field, respectively. δM (δH) represents the magnetization (magnetic field) measured from the critical value.

By defining $\delta\tilde{r}_Q(T, H) \equiv \tilde{r}_Q(T, H) - \tilde{r}_Q(0, H_t)$, we obtain

$$\chi_Q^{-1} = \delta\tilde{r}_Q(T, H) = \delta r_Q(H) + 90v(\delta\mathcal{K} + \delta\tilde{a}_0)^2, \quad (56)$$

since both $\tilde{r}_Q(0, H_t)$ and $\tilde{u}_Q(0, H_t)$ are zero at the QTCP and terms linear in $\delta\mathcal{K}$ and $\delta\tilde{a}_0$ vanish. Here δr_Q and $\delta\tilde{a}_0$ are defined as

$$\delta r_Q = r_Q(H) - r_Q(H_t) \simeq r_{QH} \delta H, \quad (57)$$

$$\delta\tilde{a}_0 = a_0^2 - a_{0t}^2 = \delta a_0(\delta a_0 + 2a_{0t}). \quad (58)$$

From eqs. (53) and (55), $\delta\mathcal{K}$ turns out to be higher order of δa_0 near the QTCP. Then, from eqs. (34) and (56), the most dominant terms of χ_Q^{-1} and χ_0^{-1} are given as

$$\chi_0^{-1} \propto \delta a_0, \quad (59)$$

$$\chi_Q^{-1} \simeq r_{QH} \delta H + 360va_{0t}^2 \delta a_0^2, \quad (60)$$

which together with eqs. (53) and (55) lead to the δH and T dependences as

$$\chi_Q^{-1} \simeq \beta_{Q0} \delta H + \beta_{Q1} T^{3/2}, \quad (61)$$

$$\chi_0^{-1} \simeq (\beta_{00} \delta H + \beta_{01} T^{3/2})^{1/2}, \quad (62)$$

$$\delta a_0 \simeq (\alpha'_0 \delta H + \alpha'_1 T^{3/2})^{1/2}. \quad (63)$$

For simpler cases of (1) $T \neq 0$ and $\delta H = 0$ (2) $T = 0$ and $\delta H \neq 0$, readers are referred to Appendix for more detailed derivations of the self-consistent procedure. Singularities of the uniform susceptibility χ_0 , the ordering susceptibility χ_Q , and the magnetization δa_0 near the QTCP are summarized in Table II. Here, we note that these critical exponents are unique and any choice of the phenomenological parameters does not change the critical exponents. These mean-field critical exponents obtained by the present SCR theory based on the classical φ^6 theory are justified in three dimensions by the following reason: It is known that the upper critical dimension d_c is three ($d_c=3$) for the φ^6 theory.¹⁹ For the quantum phase transitions, the effective dimension d_{eff} is given as $d_{\text{eff}} = d + z$, where z is the dynamical critical exponent. For the AFM QTCP, since the dynamical exponent z is two, the effective dimension d_{eff} is given as $d_{\text{eff}} = d + z = 5$, which is larger than the upper critical dimension $d_c = 3$. Therefore, the obtained critical exponents are correct in three dimensions.

4. Comparison with experimental results

We now examine whether the criticality of the QTCP is consistent with the experimental results for YbRh₂Si₂, CeRu₂Si₂, and β -YbAlB₄. In these three materials, the

convex temperature dependence of the inverse of the uniform magnetic susceptibility χ_0^{-1} ($\chi_0^{-1} \propto T^\zeta$, $\zeta < 1.0$) is observed.^{14,16,18} We again note that this convex temperature dependence of χ_0^{-1} can not be explained by the conventional ferromagnetic quantum criticality, because the critical exponent ζ is always larger than one.

For YbRh_2Si_2 , we will show that the present SCR theory reproduces quantitative behaviors of the experimental uniform magnetic susceptibility and magnetization curve by choosing the reasonable set of the phenomenological parameters. Furthermore, we show that the singularity of the QTCP is consistent with the experimental results of the specific heat, nuclear relaxation time $1/T_1T$, and Hall coefficient.

For CeRu_2Si_2 and $\beta\text{-YbAlB}_4$, we show that the singularity of the diverging enhancement of the uniform susceptibility is consistent with the quantum tricriticality. We propose a possible location of the QTCP in CeRu_2Si_2 . By fine-tuning the Rh-substitution ratio and the magnetic fields, it is possible to determine the location of the QTCP. For $\beta\text{-YbAlB}_4$, we propose that NMR study is a suitable probe to verify the prediction of our QTCP scenario.

4.1 YbRh_2Si_2

4.1.1 Experimental results of YbRh_2Si_2

At zero magnetic field ($H = 0$), it has been suggested that YbRh_2Si_2 exhibits an AFM transition at the Néel temperature $T_N = 0.07$ K.³⁵ Although neutron-scattering results are not available yet, anomalies of specific-heat and the uniform magnetic susceptibility indicate that the AFM transition actually occurs. Results of nuclear magnetic resonance (NMR)²⁴ and Mössbauer effect³⁶ also indicate the existence of the AFM order. By applying the magnetic field along the ab plane, critical temperatures of AFM transitions become zero at the critical magnetic field $H_c \sim 0.06$ T.^{14,35} For Ge-substituted $\text{YbRh}_2(\text{Si}_{0.95}\text{Ge}_{0.05})_2$, both T_N and H_c decrease to 0.02 K and 0.027 T.¹⁴ Because the AFM transitions still remain continuous one down to the lowest temperature (~ 10 m K), it has been proposed that a field-induced AFM QCP emerges. One might think that this clear QCP is a textbook example of the standard theory.⁵⁻⁸ However, its non-Fermi-liquid properties do not follow the predictions of the standard theory and are under extensive debates.²

The puzzling non-Fermi liquid behaviors observed in YbRh_2Si_2 are summarized as follows: At higher temperatures ($T > 0.3$ K), the Sommerfeld coefficient of the specific heat γ has logarithmic temperature dependence ($\gamma \propto -\log T$), while γ is increased with power laws below 0.3 K.³⁷ This behavior is not consistent with the conventional theory, in which the γ converges to a constant at low temperatures. Transport and optical data roughly show the resistivity measured from the residual resistivity ρ_0 , $\Delta\rho = \rho - \rho_0$, linearly scaled with T and frequency.^{35,38} This singularity also contradicts the prediction of the standard theory ($\Delta\rho \propto T^{3/2}$). Moreover, it has been proposed that a large change in the Hall coefficient R_H occurs near the QCP.³⁹ The most puzzling non-Fermi liquid behavior is a diverging enhancement

of the uniform susceptibility χ_0 near the AFM QTCP. The singularity of χ_0 is roughly scaled by $\chi_0 \propto T^{-\zeta}$ and $\chi_0 \propto |H - H_c|^{-\zeta'}$ with $\zeta \sim \zeta' \sim 0.6$ ¹⁴ contradicting the standard expectation of saturation to a constant. NMR²⁴ and electron spin resonance (ESR)⁴⁰ signals also indicate the enhancement of the FM susceptibility near the AFM QCP. In accordance with the diverging enhancement of the FM susceptibility, the magnetization curve has convex magnetic-field dependence.^{14,41} It has been speculated that the origin of this enhancement could be the proximity to the FM QCP.¹⁴ However, the critical exponent $\zeta \sim 0.6$ can not be explained by the standard theory, because the critical exponent ζ is always larger than one in the conventional FM QCP (see Table I). Under magnetic fields $H > H_c$, it is proposed that two characteristic energy scales exist in YbRh_2Si_2 ;⁴² one is the scale (T_{LFL}) for the establishment of the Landau Fermi liquid state, i.e., below T_{LFL} the resistivity has the Fermi-liquid form $\rho = \rho_0 + AT^2$, and the other one is the scale (T^*) where $\partial R_H/\partial H$, $\partial\rho/\partial H$, and χ_0 have peaks.

4.1.2 Choice of phenomenological parameters

In this subsection, we explain how we choose the phenomenological parameters to solve the self-consistent equations in eqs. (28), (30), (33), (34), and (35) numerically. Hereafter, for simplicity, we approximate the magnetic field dependence of $\delta r_0(H) \equiv r_0(H) - r_0(H_t)$ as $\delta r_0(H) \simeq r_{0H}\delta H$.

First, we clarify how many control parameters exist in the self-consistent equations. The four SCR parameters (T_{0A} , T_{00} , T_{QA} , and T_{Q0}) are control parameters; the five parameters (v , r_{QH} , r_{0H} , H_t , and a_{0t}) are also control parameters, whereas once these parameters are fixed, the other parameters (r_0 , r_Q , u_0 , and u_Q) are determined from the conditions $\tilde{r}_Q(0, H_t) = 0$, $\tilde{u}_Q(0, H_t) = 0$ and eqs. (30), (31). Therefore, the number of control parameters is nine in the self-consistent equations. Below we show that these parameters are required to satisfy rather strict constraint from the physical reasons.

Next, we explain how to employ a reasonable set of the control parameters. Because H_t and a_{0t} are the magnetic field and the magnetization at the QTCP, we can estimate these two parameters directly from experiments. In YbRh_2Si_2 , since we expect that H_t and a_{0t} are slightly larger than those of the QCP at ambient pressure, we choose these two parameter as $H_t = 0.08$ T and $a_{0t} = 0.2\mu_B$. According to the previous studies,⁶ it is suggested that the four SCR parameters (T_{0A} , T_{00} , T_{QA} , and T_{Q0}) have the values within the order of 10-100 K. Therefore, we choose these parameters in this range; i.e., $T_{0A} = 20$ K, $T_{00} = 10$ K, $T_{QA} = 270$ K, $T_{Q0} = 5$ K. In contrast, for the other three non-primary parameters (r_{QH} , r_{0H} , and v), we do not find any constraint from the physical requirement. Therefore, we have freely tuned these parameters to reproduce the experimental results quantitatively ($v = 21$ K, $r_{0H} = 5$, and $r_{QH} = 180$). However, the critical exponents do not change even when we have chosen these parameters arbitrarily. In Appendix, we show the details of numerical calculations. The microscopic derivation of these phenomenological parameters is left for future studies.

4.1.3 Spin fluctuations and magnetization curve

We now compare the numerical result of inverse of the uniform susceptibility χ_0^{-1} with the experimental result. As shown in Fig. 4, temperature dependence of χ_0^{-1} just above the QTCP is well consistent with experimental result. This consistency strongly supports the relevance of our proposal that the QTCP exists very close to the QCP in YbRh_2Si_2 as is shown in Fig. 3. Because the QCP in the experiment is located very close to the QTCP but slightly away from the QTCP, the nonzero offset of χ_0^{-1} exists in experiment. By approaching the QTCP, this nonzero offset becomes smaller and vanishes at the QTCP.

In the last section, we have shown that the inverse of the uniform susceptibility χ_0^{-1} scales as $T^{0.75}$ in the low-temperature limit. As a first look, this scaling at asymptotically low temperatures appears to be somewhat inconsistent with the experimental result ($\chi_0^{-1} \propto T^{0.6}$) reported in Ref. [14]. However, the numerical calculation shows that the asymptotic scaling deviates at finite temperatures and χ_0^{-1} looks nearly proportional to $T^{0.6}$ at higher temperatures ($T > 1.0\text{K}$). This is consistent with the experimental result as shown in Fig. 4.

Here, we discuss the competition between FM fluctuations and AFM fluctuations near the QTCP. As shown in Fig. 4, at high temperatures ($T > 0.6\text{K}$), the magnitude of the FM fluctuations is larger than that of the AFM fluctuations ($\chi_0 > \chi_Q$), while the magnitude of the AFM fluctuations is larger than that of the FM susceptibility at low temperatures ($T < 0.6\text{K}$). The origin of this robustness of the FM susceptibility at high temperatures is the broad structures of $\chi_{0+q}(0)$ in the wavenumber space [see eq. (45)]. We note that this competition of the spin fluctuations near the QTCP is consistent with the experimental results of the NMR study on YbRh_2Si_2 .²⁴ From the NMR study, it is proposed that the spin fluctuations are governed by the $q = 0$ FM fluctuations away from the QCP, while near the QCP, the AFM fluctuations with a finite wave number far from $q = 0$ develop significantly and governs the spin fluctuations. As we have shown here, this is indeed the tendency to be observed near QTCP.

We also note that this competition of the spin fluctuations is a possible origin of the multiple energy scales observed in YbRh_2Si_2 ^{14,42} as we mentioned in Sec. 4.1.1. In our QTCP scenario, T^* is interpreted as the energy scale where the FM fluctuation χ_0 begins to follow the Fermi-liquid form, while T_{LFL} is interpreted as the energy scale where the AFM fluctuation χ_Q begins to follow the Fermi-liquid form. Since both FM and AFM fluctuations diverge at the QTCP, two energy scales T^* and T_{LFL} become zero at the QTCP. This result is consistent with the experimental result (see Fig. 2 B in Ref. 42).

By using the same phenomenological parameters, we have also calculated the magnetization curve. As shown in Fig. 5, our result is well consistent with the experimental result in the interval of more than two orders of magnetic fields. We emphasize that the singularity of the magnetization curve ($\delta M \propto \delta H^{1/\delta}$, $\delta = 2$) can not be explained by the conventional FM quantum criticality, because the critical exponent δ must be larger than

three for the conventional FM QCP. The present critical exponent $\delta = 2$ is also completely different from that of the quantum critical end point, which belongs to the Ising universality class⁴³. For the Ising universality class, the critical exponent δ is always larger than three.

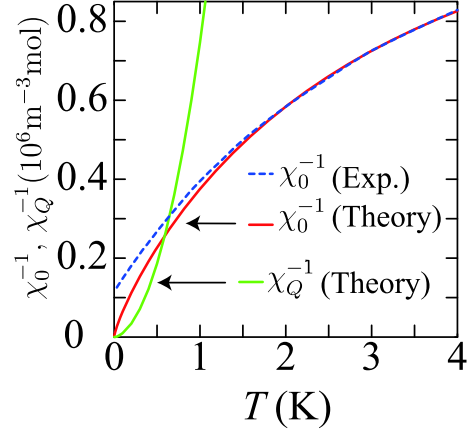


Fig. 4. (Color online) Experimental uniform magnetic susceptibility χ_0^{-1} for $\text{YbRh}_2(\text{Si}_{0.95}\text{Ge}_{0.05})_2$ at $H = 0.03$ T reported in Ref. [14] compared with numerical result of present SCR theory. Solid (red) [broken (blue)] curve represents the theoretical [experimental] χ_0^{-1} . Solid (green) curve represents the theoretical χ_Q^{-1} . The theoretical χ_0^{-1} and χ_Q^{-1} are calculated just above the QTCP ($H = H_t$).

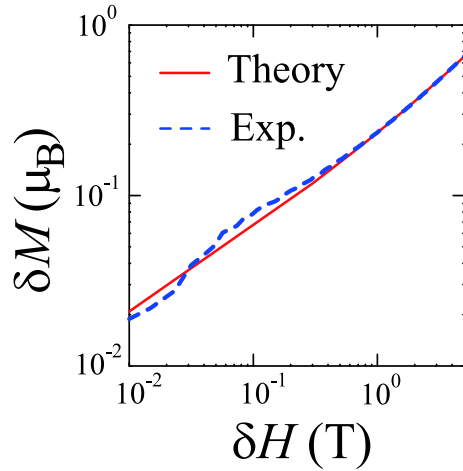


Fig. 5. (Color online) Experimental magnetization curve for $\text{YbRh}_2(\text{Si}_{0.95}\text{Ge}_{0.05})_2$ at $T = 0.09$ K reported in Ref. [14] compared with the present theory. Solid (red) [broken (blue)] curve represents the theoretical [experimental] magnetization curve. δM (δH) represents the magnetization (magnetic field) measured from the critical value. We estimate the experimental critical magnetic field H_c (magnetization M_c) as 0.027 T ($0.004 \mu_B$).

4.1.4 Specific heat

In the SCR theory, enhancement of $\chi(q, \omega)$ is the origin of the enhancement of effective mass (see Sec. 2 and Ref. [6, 30]). Near the QTCP, because $\chi(q, \omega)$ has two

peaks around $q = 0$ and $q = Q$, we can express the specific heat as

$$\begin{aligned}\gamma &= \frac{C}{T} \simeq \frac{3K_3v_0}{\pi} \int_0^{q_c} dq q^2 \int_0^\infty d\omega \frac{c(\omega)\Gamma_{Q+q}}{\omega^2 + \Gamma_{Q+q}^2} \\ &\quad + \frac{3K_3v_0}{\pi} \int_0^{q_c} dq q^2 \int_0^\infty d\omega \frac{c(\omega)\Gamma_{0+q}}{\omega^2 + \Gamma_{0+q}^2} \\ &= \gamma_Q + \gamma_0,\end{aligned}\quad (64)$$

where $c(\omega) = \omega^2 e^{\omega/T} / (T^3 (e^{\omega/T} - 1)^2)$, $\Gamma_{Q+q} = A_Q(\chi_Q^{-1}/A_Q + q^2)/C_Q$, and $\Gamma_{0+q} = A_0^{1/2}(\chi_0^{-2}/A_0 + q^2)^{1/2}q/C_0$. By substituting the numerical result of χ_Q and χ_0 into this equation, we obtain the specific heat near the QTCP as shown in Fig. 6. We note that the contribution from zero wave number (γ_0) is comparable to that of the ordering wave number (γ_Q). This indicates that the quantum tricriticality induces larger enhancement of the effective mass than that of the conventional quantum criticality. This might be the reason why YbRh₂Si₂ has larger effective mass³⁷ ($\gamma \sim 1.5 \text{ J mol}^{-1} \text{ K}^{-2}$) than those of other typical heavy-fermion compounds ($\gamma \leq 1.0 \text{ J mol}^{-1} \text{ K}^{-2}$).

Here, we discuss the obtained singularity of the Sommerfeld coefficient of the specific heat γ . At high temperatures ($T > 1.0 \text{ K}$), the singularity ($\gamma \propto -\log T$) and the amplitude are both consistent with those of the experimental result.³⁷ However, at low temperatures ($T < 1.0 \text{ K}$), within this SCR theory, the singular temperature dependence of γ is the same as that of the conventional AFM QCP ($\gamma \propto \text{const.} - T^{1/2}$), while experimentally, power-law-like behavior is observed for $T < 0.3 \text{ K}$.³⁷ In general, as long as we consider the spin fluctuations, we can not obtain the power-law divergence of the specific heat in three dimensions.

Although the clarification of the origin of this discrepancy is left for future studies, we point out the two possible origins of this discrepancy. One is the fact that the Néel temperature is actually nonzero in the experimental results. At zero magnetic field, specific heat has a sharp peak around the Néel temperature.³⁷ Remnants of this peak may be the origin of the power-law-like behavior of the specific heat at $H = 0.06 \text{ T}$. The other possible origin is effects of valence fluctuations,^{44,45} which is not considered in our spin fluctuation theory. In general, the quantum tricriticality, namely proximity to the first-order AFM transition, induces the divergence of the valence fluctuations by the following reasons: Discontinuous change in the occupations of f electrons occurs at the first-order phase transition, and at the QTCP, it is expected that the valence of f electrons changes singularly and the valence susceptibility diverges. We note that, in contrast to the pure valence transition, this divergence of the valence fluctuations is caused by the proximity to the first-order AFM transition. Therefore, in this case, the criticality of the valence fluctuations is governed by the quantum tricriticality. In other words, the Ising criticality expected from the simple valence quantum instability should not show up in this case, similarly to our statement that the uniform susceptibility does not follow the ferromagnetic criticality. However, it is expected

that contribution to the specific heat from the valence fluctuations, which is not considered in our spin fluctuation theory, explains the anomalous enhancement of γ observed in experiment.

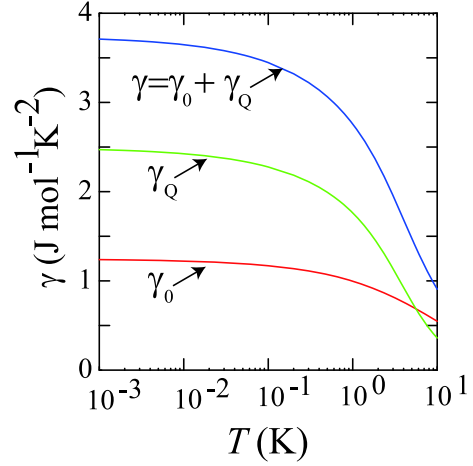


Fig. 6. (Color online) Numerical result for the Sommerfeld constant of the specific heat just above the QTCP. Here, $\gamma_Q(\gamma_0)$ represents the contributions from the ordering (zero) wave number.

4.1.5 NMR

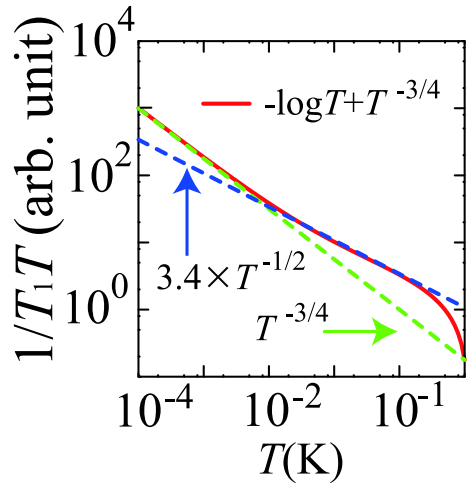


Fig. 7. (Color online) Singularity of the $1/T_1 T$ just above the QTCP. We note that $1/T_1 T$ looks proportional to $T^{-1/2}$ at the intermediate temperatures ($10^{-2} \text{ K} < T < 10^{-1} \text{ K}$). Near the QCP in YbRh₂Si₂, $1/T_1 T$ appears to be proportional to $T^{-1/2}$.²⁴ This behavior is consistent with the quantum tricriticality.

In this section, we consider the singularity of the nuclear relaxation time $1/T_1 T$ near the QTCP. As we have mentioned in Sec. 2, the singularity of $1/T_1 T$ is scaled with the spin fluctuations.^{31,32} By using the conventional relation, we obtain the singularity of $1/T_1 T$ near the

QTCP as

$$\begin{aligned} \frac{1}{T_1 T} &= \frac{2\gamma_N^2}{N_0} \sum_q \lim_{\omega \rightarrow 0} \frac{\text{Im}\chi^{-+}(q, \omega)}{\omega} \\ &\propto \left(\int_0^{q_c} dq |A_{0+q}|^2 \frac{\chi_{0+q}}{\Gamma_{0+q}} + \int_0^{q_c} dq |A_{Q+q}|^2 \frac{\chi_{Q+q}}{\Gamma_{Q+q}} \right) \\ &\sim -D_0 \log T + D_Q T^{-3/4}, \end{aligned} \quad (65)$$

where γ_N is a gyromagnetic ratio and A_q is the q component of hyper-fine couplings; D_0 and D_Q are constants.

We note that the contributions from FM susceptibility induce the unconventional logarithmic temperature dependence of $1/T_1 T$. Because it is difficult to determine the value of A_Q and A_0 quantitatively, we do not calculate to show quantitative behavior of the $1/T_1 T$. Alternatively, in Fig. 7 (a), we show a qualitative behavior of $1/T_1 T$ by simply taking $D_0 = D_Q = 1$. Because the subdominant term $-\log T$ exists, $1/T_1 T$ does not follow the dominant temperature dependence $T^{-3/4}$ at high temperatures ($T > 10^{-2}$ K) but seems to be proportional to $T^{-1/2}$ at the intermediate temperatures. This behavior is consistent with the unconventional temperature dependence ($1/T_1 T \propto T^{-1/2}$) observed in YbRh_2Si_2 .²⁴

4.1.6 Hall coefficient

In this section, we show that the singularity of the Hall coefficient can be explained by the quantum tricriticality. According to the Coleman's simple argument in Ref. [46], the Hall coefficient R_H is proportional to the square of the order parameter ($R_H \propto M^2$). Near the QTCP, the order parameter is proportional to $|g - g_c|^{1/4}$ (see Refs. [19, 20]), where g (g_c) is the (critical value of) control parameter. Therefore, Hall coefficient is scaled with $|g - g_c|^{1/2}$ near the QTCP. This result indicates that the Hall coefficient changes non-analytically near the QTCP. Moreover, if the QCP in YbRh_2Si_2 is located slightly away from the QTCP but on the side of weak first-order phase transitions, the Hall coefficient must change discontinuously with a jump. These behaviors are consistent with the experimental results.³⁹

We note that the above argument is qualitative. To clarify the change in the Hall coefficient quantitatively, it is necessary to consider the realistic band structures of YbRh_2Si_2 . By calculating the band structures of YbRh_2Si_2 , Norman⁴⁷ has pointed out that small changes of the f electron occupation are sufficient to reproduce the experimental result. In general, proximity to the first-order transition indeed induces such changes of the f electron occupation near the QTCP. Although it is intriguing to perform detailed calculations of the Hall coefficient based on the microscopic band structures combined with the quantum tricriticality, such treatment is beyond the scope of the present paper.

4.2 CeRu_2Si_2

CeRu_2Si_2 is a canonical heavy-fermion system, which has no apparent magnetic order and shows a large Sommerfeld coefficient $\gamma \sim 360 \text{ mJ/molK}^2$.^{48, 49} The result of the neutron scattering shows that AFM spin correlation

develops below 60K,⁵⁰ and detailed inelastic neutron-scattering study shows that the spin fluctuations can be explained by the conventional SCR theory.⁵¹ By substituting Ru (Ce) with Rh (La) slightly,^{18, 52} AFM long-range order emerges. From these experimental results, it is recognized that CeRu_2Si_2 is located very close to the AFM QCP. We note that, although no clear evidence of magnetic long-range order was observed by the measurement of the bulk properties, ultrasmall ordered moment ($\sim 10^{-3} \mu_B/\text{Ce}$) was detected by μSR below 0.1K.⁵³

In CeRu_2Si_2 , specific heat, resistivity, and uniform magnetic susceptibility do not show non-Fermi liquid behaviors down to 20mK. However, below 20mK, non-Fermi liquid behavior is observed. Actually, as shown in Fig. 8, Takahashi *et al.* have found a diverging enhancement of the uniform magnetic susceptibility at temperatures of micro Kelvin order.¹⁵ In the same temperature range, Yoshida *et al.* have found that thermal expansion and magnetostriction also show non-Fermi liquid behaviors.⁵⁴ By fitting the uniform magnetic susceptibility with the function $\chi_0^{-1} = aT^\zeta$, we estimate the critical exponent ζ as ~ 0.53 . This value of ζ is close to that of the QTCP, and is not explained by the conventional quantum criticality. Therefore, it is plausible that this diverging enhancement is caused by the proximity effect of the QTCP.

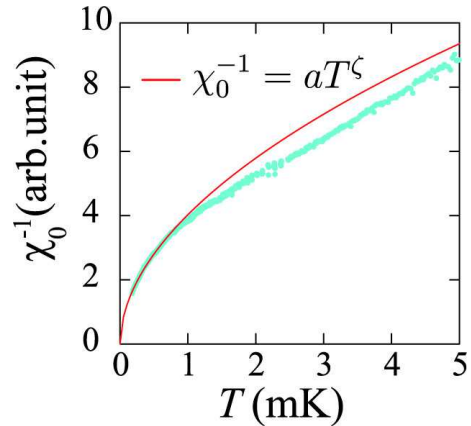


Fig. 8. (Color online) Experimental χ_0^{-1} for CeRu_2Si_2 at low temperatures reported in Ref. [15]. The solid line shows the result of a least-square fitting by assuming the function $\chi_0^{-1} = aT^\zeta$, where a is a constant. We estimate the critical exponent ζ as $\zeta \sim 0.53$.

We now discuss where the QTCP is located in CeRu_2Si_2 . In Rh-substituted compound $\text{Ce}(\text{Ru}_{1-x}\text{Rh}_x)_2\text{Si}_2$, it is known that the AFM magnetic order occurs for $x > 0.03$. At $x=0.1$, it was shown that the slope of the magnetization curve becomes steeper by lowering temperatures (see Fig. 9 in Ref. [18]). This experimental result indicates that the continuous AFM phase transitions changes into the first-order ones at low temperatures, and between them TCP exists at finite temperatures, where the slope of the magnetization is supposed to diverge. We show the expected phase diagram for $x = 0.1$ in Fig. 9(a). We note that this

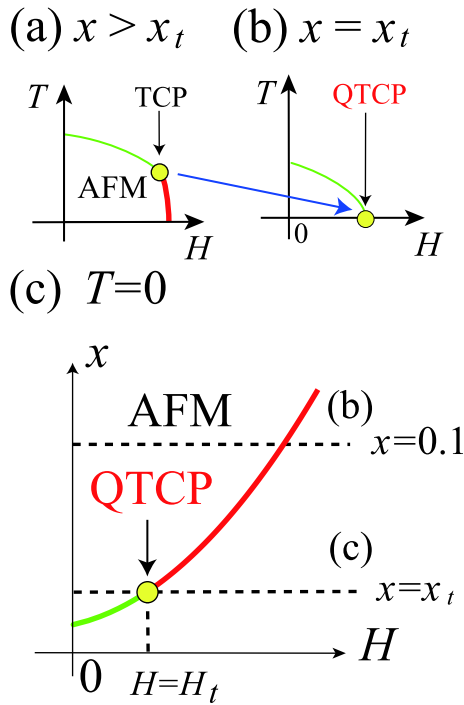


Fig. 9. (Color online)(a) Phase diagram of $\text{Ce}(\text{Ru}_{1-x}\text{Rh}_x)_2\text{Si}_2$ for $x > x_t$. Here, x_t is the critical substituting ratio where the critical temperatures of the TCP becomes zero. (b) Phase diagram of $\text{Ce}(\text{Ru}_{1-x}\text{Rh}_x)_2\text{Si}_2$ at $x = x_t$. At this substituting ratio, the QTCP appears at $H = H_t$. (c) Expected phase diagram of $\text{Ce}(\text{Ru}_{1-x}\text{Rh}_x)_2\text{Si}_2$ at zero temperatures. The QTCP appears at $(x, H) = (x_t, H_t)$.

first-order magnetic phase transition is *not* related with the metamagnetic transitions at $H_M \sim 8\text{T}$ observed in pure CeRu_2Si_2 . The remnant of this metamagnetic phase transition still survives at $x = 0.1$ around $H \sim 6\text{T}$. By decreasing the substitution ratio x , it is expected that the critical temperatures of the TCP become zero at the critical substitution ratio x_t and QTCP emerges as is shown in Fig. 9(b). We show the expected ground-state phase diagram of $\text{Ce}(\text{Ru}_{1-x}\text{Rh}_x)_2\text{Si}_2$ in Fig. 9(c). Similarly to YbRh_2Si_2 , because the QTCP is very close to $x = 0.0$ and $H = 0.0$, the diverging enhancement of χ_0 is observed in pure CeRu_2Si_2 .

Here, we comment on the singularities of other physical properties (specific heat, nuclear magnetic relaxation time, and Hall coefficient), which are discussed for YbRh_2Si_2 . In these physical properties, it is expected that the same singularities as those of YbRh_2Si_2 are observed in CeRu_2Si_2 , because the criticality of the QTCP does not depend on the details of materials.

Compared with YbRh_2Si_2 , the occurrence of the diverging enhancement of χ_0 is suppressed to very low temperatures ($T < 20\text{mK}$) in CeRu_2Si_2 . Although the criticality of the QTCP accounts for the singularity of χ_0 qualitatively, it does not explain the origin of this suppression. Clarifying the origin of this suppression is left for future studies.

To summarize, in CeRu_2Si_2 , QTCP is expected to exist very close to the ambient pressure and the zero magnetic field, and quantum tricriticality is the origin of the

anomalous diverging enhancement of the uniform magnetic susceptibility. It is highly desirable to determine the location of the QTCP precisely by fine-tuning the Rh-substitution ratio x and the magnetic field H .

4.3 $\beta\text{-YbAlB}_4$

$\beta\text{-YbAlB}_4$ is a newly discovered heavy-fermion compound, which has a large Sommerfeld coefficient $\gamma \sim 300\text{mJ/molK}^2$.⁵⁵ In this material, up to now, neither apparent QCP nor magnetic order have been found at ambient pressure. However, the superconducting transition with $T_c = 80\text{mK}$ is found.^{16, 56}

In $\beta\text{-YbAlB}_4$, the non-Fermi liquid behaviors are observed at ambient pressure. The striking feature of $\beta\text{-YbAlB}_4$ is the divergence of the uniform magnetic susceptibility ($\chi_0 \propto T^{-\zeta}$, $\zeta = 1/3$).¹⁶ Because the critical exponent ζ is smaller than one, we can exclude the possibility that this divergence is caused by the FM QCP. However, this critical exponent $\zeta = 1/3$ is substantially smaller than that of the QTCP. If this value $1/3$ is correct, a possible origin of this discrepancy is the low dimensionality. From the crystal structures,⁵⁵ it is expected that this material has one dimensional anisotropy. This low dimensionality may modify the criticality of the QTCP at high temperatures ($T \gg 0.1\text{K}$). However, the criticality is expected to follow that of the three dimensionality at sufficiently low temperatures ($T \ll 0.1\text{K}$). We expect such a crossover to occur at lower temperatures below 0.1K .

Here, we explain why the low dimensionality makes the critical exponent ζ small. From eq. (15), critical exponent of the order-parameter fluctuations becomes smaller by lowering the dimensions (see also Table I). Therefore the critical exponent ζ , which is scaled with half of the critical exponents of the order-parameter fluctuations, also becomes smaller by lowering the dimensions.

If the AFM QTCP exists around the ambient pressure and the zero magnetic field in $\beta\text{-YbAlB}_4$, coexistence of the enhanced AFM and FM fluctuations are expected to be observed (see Sec. 4.1.3). By performing the NMR measurement, it is possible to detect such coexistence of spin fluctuations as is observed in YbRh_2Si_2 .²⁴

5. Summary and Discussion

In this paper, quantum tricriticality has been studied by extending the conventional SCR theory. Near the AFM QTCP, not only the AFM fluctuations but also the FM fluctuations show diverging enhancement. By considering the combined effects of these two different diverging fluctuations, we have shown that unconventional non-Fermi-liquid behaviors appear around the QTCP. We have proposed that the quantum tricriticality explains the unconventional quantum criticality observed in YbRh_2Si_2 , CeRu_2Si_2 , and $\beta\text{-YbAlB}_4$.

In YbRh_2Si_2 , as we have explained in Sec. 4.1, available experimental results strongly support the existence of the QTCP under pressure. Actually, we have shown that the quantum tricriticality is consistent with the puzzling quantum criticality observed in YbRh_2Si_2 .

More concretely, near the AFM QTCP, we have clarified singularity of the uniform magnetic susceptibil-

ity as $\chi_0 \propto T^{-3/4}$ at low temperatures. We have also clarified the singularity of the magnetization curve as $\delta M \propto \delta H^{1/2}$. It is noteworthy that these critical exponents are completely different from the conventional quantum criticality (see Table I), and are consistent with the experimental results of YbRh_2Si_2 . Furthermore, for the magnetic susceptibility and the magnetization curve, by solving the self-consistent equations numerically, we have shown that the quantum tricriticality is consistent with the experimental results of YbRh_2Si_2 not only qualitatively but also quantitatively. This includes a crossover from $\chi_0 \propto T^{-3/4}$ to $\chi_0 \sim T^{-0.6}$ at elevated temperatures.

On the Sommerfeld constant of the specific heat γ , we have shown that the singularity ($\gamma \propto -\log T$) and the amplitude are both consistent with those of the experimental result³⁷ at high temperatures ($T > 1.0\text{K}$). Especially, near the QTCP, we have shown that the contribution from the uniform magnetic susceptibility plays an important role in making the heavy quasiparticles. However, at low temperatures ($T < 1.0\text{K}$), within our theory, γ converges to a constant ($\gamma \propto \text{const.} - T^{1/2}$), while experimentally, a power-law-like behavior is observed for $T < 0.3\text{K}$.³⁷ This discrepancy may be solved by considering either the fact that the Néel temperature is actually nonzero or effects of valence fluctuations.^{44,45} In our point of view, contribution from the valence fluctuations is the most promising candidate to explain the anomalous enhancement of effective mass. It is an intriguing challenge to extend the present spin fluctuation theory to treat the interplay between spin and charge fluctuations such as valence fluctuations.

The quantum tricriticality also induces unconventional behavior of the nuclear relaxation time, namely $1/T_1T$. Near the QTCP, we have shown that the $1/T_1T$ is proportional to $-D_0 \log T + D_Q T^{-3/4}$, where D_0 and D_Q are constants. Due to the existence of a logarithmic divergence, temperature dependence of the $1/T_1T$ seems to be weaker than $T^{-3/4}$ at high temperatures. Thus, at intermediate temperatures, we have shown that $1/T_1T$ seems to be proportional to $T^{-1/2}$. This behavior is consistent with the experimental results of YbRh_2Si_2 .²⁴

We have also shown that the large change in the Hall coefficient³⁹ can be well accounted for by the quantum tricriticality. In this paper, we only consider the qualitative aspect of the Hall coefficient. It is left for future study to clarify the quantitative changes of the Hall coefficient near the QTCP.

Here, we comment on singularities of the resistivity. In the quantum tricritical scenario, if we consider the singularity of the relaxation time only, the singular temperature dependence of the resistivity is the same as that of the conventional three dimensional AFM QCP, i.e., $\rho \propto T^{3/2}$. This is inconsistent with the linear-like temperature dependence of the resistivity observed in experiment.³⁷ However, according to the simple Drude picture, the resistivity ρ is proportional not only to the relaxation time τ but also to the carrier density n , i.e., $\rho \propto 1/n\tau$. Near the QTCP, it is expected that the carrier density also has the singularity. If its singularity is the same as that of the magnetization, we obtain the singularity of

the resistivity as $\rho \propto T^{3/2}/(n_0 + n_1 T^{3/4})$, where n_0 and n_1 are constants. This singularity of the resistivity may explain the linear-like temperature dependence of the resistivity observed in the experiments. To examine the validity of the above simple arguments, further studies are desirable.

As we have explained above, many of unconventional behaviors of YbRh_2Si_2 can be accounted by the quantum tricriticality. In fact, we do not find any experimental results of YbRh_2Si_2 that explicitly contradict our theory. We emphasize that no other theory in the literature is able to explain the anomalous quantum criticality observed in YbRh_2Si_2 such as the coexistence of the enhanced AFM and FM fluctuations, and the criticality of the uniform susceptibility. Although these results ensure the relevance of our theory, further experimental study to determine the precise location of the QTCP by tuning the pressure and the magnetic field will be a crucial test of our theory.

Here, we comment on three different scenarios proposed for the QCP in YbRh_2Si_2 ; local quantum criticality,^{46,57} reconstruction of the Fermi surface,⁵⁸ and fermion condensate.⁵⁹

In the local quantum critical scenario, Coleman *et al.* claim that a breakdown of a composite heavy fermion (namely, all f electrons decouple from the Fermi surface) occurs at the AFM QCP. In a simple interpretation, their scenario indicates that no heavy electron exists in the ordered phase any more. Thus, their scenario seems to be inconsistent with the large Sommerfeld coefficient of the specific heat observed in the ordered phase.³⁷ Although they claim that the dynamical Kondo correlations in the ordered phase can account for the heavy electrons,^{3,60} to the authors' knowledge, there are no quantitative calculations to be compared with the experimental results. It is desirable to examine whether a large Sommerfeld coefficient of the specific heat γ observed even in the ordered phase can be quantitatively reproduced in the local quantum critical scenario.

We now examine the experimental evidence of the local quantum criticality. It has been proposed that a large change in the Hall coefficient in YbRh_2Si_2 ³⁹ is the evidence of the local quantum criticality. However, as we examined in Sec. 4.1.6, quantum tricriticality naturally explains such a large change in the Hall coefficient qualitatively. Therefore, the large change in the Hall coefficient is not a conclusive evidence of their scenario. The singularity of the nuclear magnetic relaxation time $1/T_1T$ is given as $1/T_1T \propto T^{-1}$ in their local quantum critical scenario (see eq. (4) in Ref. [57]). We emphasize that this behavior is *not* consistent with the experimental result of the NMR measurement.²⁴ The local quantum critical scenario also claims that the susceptibility follows the ω/T scaling.⁵⁷ Although this behavior is observed in $\text{CeCu}_{5.9}\text{Au}_{0.1}$ ⁶¹, it is not clear whether this behavior can be observed in YbRh_2Si_2 because the neutron-scattering results are not available yet. In contrast to their scenario, our theory predicts the conventional $\omega/T^{3/2}$ scaling.⁶ Further experiments are desirable to examine which behavior is observed in YbRh_2Si_2 .

Here, we note that the unconventional quantum criti-

cality observed in $\text{CeCu}_{5.9}\text{Au}_{0.1}$ is qualitatively different from that of the YbRh_2Si_2 . In particular, no diverging enhancement of the uniform magnetic susceptibility is observed and no clear evidence of the first-order transition is found. Therefore, quantum tricriticality is not an origin of the unconventional quantum criticality observed in $\text{CeCu}_{5.9}\text{Au}_{0.1}$. Although the local quantum criticality can explain the inelastic neutron-scattering result⁶¹ and large changes in the Hall coefficient,⁶² it can not explain all the experimental results. For example, singularity of the nuclear magnetic relaxation time $1/T_1T$ does not simply follow the prediction of the local quantum criticality.^{63,64} Furthermore, by changing the Au substitution ratio slightly, it has shown that inelastic neutron-scattering result is described better by the conventional $\omega/T^{3/2}$ scaling than by the ω/T scaling.⁶⁵ These experimental results indicates that the local quantum criticality is insufficient for explaining the unconventional quantum criticality of $\text{CeCu}_{5.9}\text{Au}_{0.1}$. Further studies are needed to clarify the origin of the unconventional quantum criticality observed in $\text{CeCu}_{5.9}\text{Au}_{0.1}$.

Next, we comment on the Fermi-surface reconstruction scenario. By using the variational Monte Carlo method, Watanabe and Ogata⁵⁸ claim that the first-order AFM transition accompanied by the changes in a Fermi-surface topology occur in the two-dimensional Kondo lattice model. Their scenario is different from the local quantum criticality in the sense that the Kondo screening still remains even in the AFM phase. They also claim that this first-order phase transition is the possible origin of the large change in the Hall coefficient observed in YbRh_2Si_2 . Their scenario has similarity with our quantum tricritical scenario on the point that the proximity to the first-order phase transition induces the large change in the Hall coefficient. However, we note that the experimental large change in the Hall coefficient is observed near the continuous phase transition. Therefore, it is not clear whether the nature of this first-order phase transition can explain the experimental large change in the Hall coefficient. Further study on the interplay between the changes in Fermi-surface topology, i.e., Lifshitz transitions⁶⁶⁻⁷⁰ and the quantum tricriticality is a challenging issue for the future.

In the fermion-condensate scenario,⁵⁹ by assuming the divergence of the effective mass, it is shown that both the FM susceptibility χ_0 and the Sommerfeld coefficient of the specific heat γ diverge with the singularity $T^{-2/3}$. They proposed that this singularity is consistent with the experimental results of YbRh_2Si_2 and CeRu_2Si_2 . Although their theory has succeeded in explaining the experimental results, it is not clear why the effective mass diverges at the AFM QCP. Furthermore, we point out that their theory does not explain why the FM and AFM fluctuations coexist as observed in YbRh_2Si_2 .

In Sec. 4.2, we have pointed out that the quantum tricriticality can be observed in CeRu_2Si_2 . In CeRu_2Si_2 , the diverging enhancement of the FM susceptibility χ_0 is observed at very low temperatures.¹⁵ We have shown that the singularity of χ_0 is qualitatively consistent with the criticality of the QTCP. This result indicates that the QTCP is located very close to pure CeRu_2Si_2 . For the

Rh-substituted compound $\text{Ce}(\text{Ru}_{1-x}\text{Rh}_x)_2\text{Si}_2$, we predict that the AFM TCP exists under magnetic field at $x = 0.1$. By decreasing the substitution ratio x , it is expected that the critical temperatures of TCP becomes zero and the QTCP appears at the critical substitution ratio x_t (see Fig. 9). CeRu_2Si_2 appears to be a suitable material to search for the QTCP, because large single crystals are available and precise measurements are possible.

In Sec. 4.3, we have proposed that the quantum tricriticality is the possible origin of the diverging enhancement of χ_0 observed in $\beta\text{-YbAlB}_4$. Although the convex temperature dependence of χ_0^{-1} is consistent with the criticality of the QTCP, the critical exponent $\zeta = 1/3$ is much smaller than that of the QTCP. We have pointed out that a possible origin of this discrepancy is the low dimensionality of $\beta\text{-YbAlB}_4$. It is left for future studies to clarify how the low dimensionality affects the criticality of the QTCP at finite temperatures.

We now discuss the singularities of the FM susceptibility around the conventional AFM QCP. Based on the conventional SCR theory, Hatatani, Narikiyo, and Miyake clarified the singularity of the FM susceptibility around the AFM QCP at zero magnetic field with the dynamical exponent $z = 2$ as well as $z = 3$.⁷¹ They showed that the singularity of χ_0 is given as $\chi_0 \sim a - bT^{1/4}$ ($\chi_0 \sim a - bT^{1/3}$) for $z = 2$ ($z = 3$) AFM QCP, where a and b are constants. They proposed that such singularity is consistent with the experimental result of Ce_7Ni_3 .⁷² By using the renormalization-group theory, Fischer and Rosch proposed that the FM susceptibility has the similar singularity around the AFM QCP under magnetic fields.⁷³ We note that these theories are only applicable to the continuous quantum phase transitions, and do not reproduce the diverging enhancement of the FM susceptibility observed in YbRh_2Si_2 , CeRu_2Si_2 , and $\beta\text{-YbAlB}_4$.

Finally, we discuss broader implications of the quantum tricriticality for the other fields of condensed matter physics. We have applied the theory of quantum tricriticality specifically to typical f electron systems with large effective masses. However, it should be noted that the present theory offers a general framework which may be applied to systems other than the heavy fermion compounds. The quantum tricriticality is significant in several different fields of condensed matter physics and will attract much interests from experimentalists as well as from theorists, because the TCP is known to play important roles in various fields of physics, for instance, in the problem for the mixture of ^3He and ^4He ⁷⁴ as is studied by using Blume-Emery-Griffiths model.⁷⁵ Recently, it has also been proposed that the TCP plays an important role on ultracold atomic Fermi gases.⁷⁶ Therefore, it is a highly fundamental issue how the tricritical phenomena are modified when quantum fluctuations drives the critical point to zero temperature. It is desirable to explore the novel phenomena such as unconventional superconductivity induced by the quantum tricriticality.

Acknowledgements

The authors would like to thank Haruhiko Suzuki for sending us their experimental data on CeRu_2Si_2 and

also thank fruitful discussions. This work is supported by Grant-in-Aid for Scientific Research (grant numbers 17071003 and 16076212) from MEXT, Japan. YY are supported by the Japan Society for the Promotion of Science.

Appendix: Details of the numerical calculations for the self-consistent equations

In this appendix, we show the details of the numerical calculations for the self-consistent equations for the QTCP given in Sec. 3. For simplicity, we only consider the solutions for two cases; (1) $T \neq 0$ and $\delta H = 0$, and (2) $T = 0$ and $\delta H \neq 0$.

(1) $T \neq 0$ and $\delta H = 0$

First, to determine the singularities of the physical properties, we will obtain the five self-consistent equations given in (A.1)-(A.5). By solving eq. (54), we obtain the singularity of δa_0 as

$$\delta a_0 = \frac{-B + (B^2 - 4A_t C)^{1/2}}{2A_t}, \quad (\text{A}\cdot 1)$$

where we approximate $A = 12a_{0t}(5va_{0t}^2 + \tilde{u}_0)$ as $A \simeq A_t = 12\tilde{u}_0 a_{0t} + 60va_{0t}^3$, and B (C) is defined as $B = \delta\tilde{r}_0 + 12a_{0t}^2\delta\tilde{u}_0$ ($C = a_{0t}\delta\tilde{r}_0 + 4a_{0t}^3\delta\tilde{u}_0 - \delta H$). From eq. (56), we obtain the singularity of χ_Q^{-1} as

$$\chi_Q^{-1} = \delta\tilde{r}_Q(T, H) = \delta r_Q(H) + 90v(\delta\mathcal{K} + \delta\tilde{a}_0)^2. \quad (\text{A}\cdot 2)$$

We also obtain the singularity of $\delta\mathcal{K}$ as

$$\delta\mathcal{K} = -K_{01}\chi_0^{-2} - K_{Q1}\chi_Q^{-1} + \mathcal{K}_0(T) + \mathcal{K}_Q(T). \quad (\text{A}\cdot 3)$$

By differentiating eq. (54) with respect to the magnetic field H , we obtain the singularity of χ_0 as

$$\begin{aligned} \chi_0 &= -\frac{\frac{\partial B}{\partial H}\delta a_0 + \frac{\partial C}{\partial H}}{2\delta a_0 A_t + B} \\ &= M_1 \frac{\partial\delta\mathcal{K}}{\partial H} + M_2, \end{aligned} \quad (\text{A}\cdot 4)$$

where

$$\begin{aligned} M_1 &= -[(180v\delta\mathcal{K} + A_t/a_{0t} + 120va_{0t}^2) \\ &\quad \delta a_0 + A_t + 180va_{0t}]/(2\delta a_0 A_t + B), \\ M_2 &= -(r_{0H}\delta a_0 + a_{0t}r_{0H} - 1)/(2\delta a_0 A_t + B). \end{aligned}$$

Here, we note that χ_0 depends on $\partial\delta\mathcal{K}/\partial H$ explicitly. To obtain the explicit form of the $\partial\delta\mathcal{K}/\partial H$, we differentiate $\delta\mathcal{K}$ with respect H ;

$$\begin{aligned} \frac{\partial\delta\mathcal{K}}{\partial H} &= -K_{01} \frac{\partial\chi_0^{-2}}{\partial H} + \frac{\partial\chi_0^{-2}}{\partial H} \frac{\partial\mathcal{K}_0(T)}{\partial\chi_0^{-2}} \\ &\quad - K_{Q1} \frac{\partial\chi_Q^{-1}}{\partial H} + \frac{\partial\chi_Q^{-1}}{\partial H} \frac{\partial\mathcal{K}_Q(T)}{\partial\chi_Q^{-1}} \\ &\simeq -B_0(K_{01} - \frac{\partial\mathcal{K}_0(T)}{\partial\chi_0^{-2}}) - B_Q(K_{Q1} - \frac{\partial\mathcal{K}_Q(T)}{\partial\chi_Q^{-1}}), \end{aligned} \quad (\text{A}\cdot 5)$$

where we approximate $\partial\chi_0^{-2}/\partial H$ and $\partial\chi_Q^{-1}/\partial H$ as their values in the low-temperature limit, i.e., B_0 and B_Q are

defined as

$$\begin{aligned} B_0 &= \lim_{T \rightarrow 0} \left. \frac{\partial\chi_0^{-2}}{\partial H} \right|_{\delta H=0}, \\ B_Q &= \lim_{T \rightarrow 0} \left. \frac{\partial\chi_Q^{-1}}{\partial H} \right|_{\delta H=0}. \end{aligned}$$

B_0 and B_Q can be determined from eqs. (A.1)-(A.4). By solving eqs. (A.1)-(A.5), we can determine the singularity of χ_0^{-1} , χ_Q^{-1} , δa_0 , $\delta\mathcal{K}$, and $\partial\delta\mathcal{K}/\partial H$. Concrete procedure is shown in Fig. A.1.

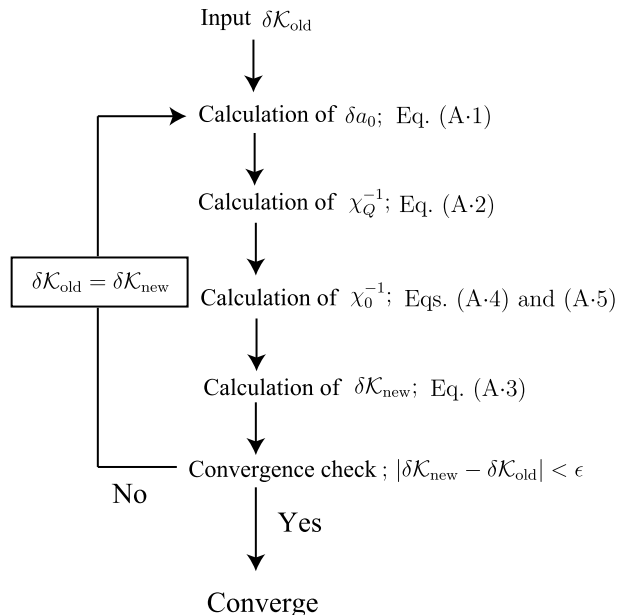


Fig. A.1. Schematic diagram for calculating self-consistent equations given in eqs. (A.1)-(A.5). Here, ϵ is the criterion for the convergence.

(2) $T = 0$ and $\delta H \neq 0$

At zero temperature, from eq. (A.3), we can easily express χ_0 as a function of $\delta\mathcal{K}$ because both $\mathcal{K}_0(0)$ and $\mathcal{K}_Q(0)$ are zero;

$$\chi_0^{-1} = \left(-\frac{\delta\mathcal{K} + K_{Q1}\chi_Q^{-1}}{K_{01}}\right)^{1/2}. \quad (\text{A}\cdot 6)$$

We note that χ_0^{-1} only depends on $\delta\mathcal{K}$ and δH , because χ_Q^{-1} is the function of $\delta\mathcal{K}$ and δH (see eqs. (A.1) and (A.2)). Therefore, by using eqs. (A.4) and (A.6), we obtain the differential equation with respect $\delta\mathcal{K}$ as

$$\begin{aligned} \frac{\partial\delta\mathcal{K}}{\partial H} &= (\chi_0 - M_2)/M_1 \\ &= f(\delta\mathcal{K}, \delta H), \end{aligned} \quad (\text{A}\cdot 7)$$

where the function f only depends on the $\delta\mathcal{K}$ and δH , because M_1 and M_2 only depends on the $\delta\mathcal{K}$ and δH . By solving this differential equation, we obtain the magnetic field dependence of physical properties at zero temperature.

- 2) H. v. Löhneysen, A. Rosch, M. Vojta, and P. Wölfle: *Rev. Mod. Phys.* **79** (2007) 1015.
- 3) P. Gegenwart, Q. Si, and F. Steglich: *Nature Phys.* **4** (2008) 186.
- 4) S. Doniach, *Physica B+C*: **91** (1977) 231.
- 5) J. A. Hertz: *Phys. Rev. B* **14** (1976) 1165.
- 6) T. Moriya: *Spin Fluctuations in Itinerant Electron Magnetism* (Springer-Verlag, Berlin, 1985).
- 7) T. Moriya and T. Takimoto: *J. Phys. Soc. Jpn* **64** (1995) 960.
- 8) A. J. Millis: *Phys. Rev. B* **48** (1993) 7183.
- 9) S. Takashima, M. Nohara, H. Ueda, N. Takeshita, C. Terakura, F. Sakai, and H. Takagi: *J. Phys. Soc. Jpn* **76** (2007) 043704.
- 10) C. Pfleiderer, P. Böni, T. Keller, U. K. Rößler, and A. Rosch: *Science* **316** (2007) 1871.
- 11) N. Takeshita, S. Takashima, C. Terakura, H. Nishikubo, S. Miyasaka, M. Nohara, Y. Tokura, and H. Takagi: arXiv:0704.0591 (2007).
- 12) R. A. Borzi, S. A. Grigera, J. Farrell, R. S. Perry, S. J. S. Lister, S. L. Lee, D. A. Tennant, Y. Maeno, A. P. Mackenzie: *Science* **315** (2007) 214.
- 13) S. S. Saxena, P. Agarwal, K. Ahilan, F. M. Grosche, R. K. W. Haselwimmer, M. J. Steiner, E. Pugh, I. R. Walker, S. R. Julian, P. Monthoux, G. G. Lonzarich, A. Huxley, I. Sheikin, D. Braithwaite, and J. Flouquet: *Nature* **406** (2000) 587.
- 14) P. Gegenwart, J. Custers, Y. Tokiwa, C. Geibel, and Steglich: *Phys. Rev. Lett.* **94** (2005) 076402.
- 15) D. Takahashi, S. Abe, H. Mizuno, D. A. Tayurskii, K. Matsumoto, H. Suzuki, and Y. Ōnuki: *Phys. Rev. B* **67** (2003) 180407(R).
- 16) S. Nakatsuji, K. Kuga, Y. Machida, T. Tayama, T. Sakakibara, Y. Karaki, H. Ishimoto, S. Yonezawa, Y. Maeno, G. G. Lonzarich, L. Balicas, H. Lee, and Z. Fisk: *Nature Physics* **4** (2008) 603.
- 17) G. Knebel, R. Boursier, E. Hassinger, G. Lapertot, P. G. Niklowitz, A. Pourret, B. Salce, J. P. Sanchez, I. Sheikin, P. Bonville, H. Harima, and J. Flouquet: *J. Phys. Soc. Jpn* **75** (2006) 114709.
- 18) C. Sekine, T. Sakakibara, H. Amitsuka, Y. Miyako, and T. Goto: *J. Phys. Soc. Jpn* **61** (1992) 4536.
- 19) For a review, I. D. Lawrie and S. Sarbach: *Phase Transitions and Critical Phenomena*, ed. by C. Domb and J. L. Lebowitz (Academic Press, London, 1984), Vol. 9, p. 2.
- 20) T. Misawa, Y. Yamaji, and M. Imada: *J. Phys. Soc. Jpn.* **75** (2006) 064705.
- 21) T. Misawa, Y. Yamaji, and M. Imada: *J. Phys. Soc. Jpn.* **77** (2008) 093712.
- 22) J. Schmalian, and M. Turlakov: *Phys. Rev. Lett.* **93** (2004) 036405.
- 23) A. G. Green, S. A. Grigera, R. A. Borzi, A. P. Mackenzie, R. S. Perry, and B. D. Simons: *Phys. Rev. Lett.* **95** (2005) 086402.
- 24) K. Ishida, K. Okamoto, Y. Kawasaki, Y. Kitaoka, O. Trovarelli, C. Geibel, and F. Steglich: *Phys. Rev. Lett.* **89** (2002) 107202.
- 25) T. Moriya and A. Kawabata: *J. Phys. Soc. Jpn* **34** (1973) 639.
- 26) T. Moriya and A. Kawabata: *J. Phys. Soc. Jpn* **35** (1973) 669.
- 27) H. Hasegawa and T. Moriya: *J. Phys. Soc. Jpn* **36** (1974) 1542.
- 28) T. Moriya and K. Ueda: *Adv. Phys.* **49** (2000) 555.
- 29) R. Kubo: *J. Phys. Soc. Jpn.* **12** (1957) 570.
- 30) A. Ishigaki and T. Moriya: *J. Phys. Soc. Jpn.* **68** (1998) 3673.
- 31) T. Moriya: *Prog. Theor. Phys.* **16** (1956) 23.
- 32) T. Moriya: *J. Phys. Soc. Jpn* **18** (1963) 4.
- 33) K. Ueda and T. Moriya: *J. Phys. Soc. Jpn* **39** (1975) 605.
- 34) K. Ueda: *J. Phys. Soc. Jpn* **43** (1977) 1497.
- 35) O. Trovarelli, C. Geibel, S. Mederle, C. Langhammer, F. M. Grosche, P. Gegenwart, M. Lang, G. Sparn, and F. Steglich: *Phys. Rev. Lett.* **85** (2000) 626.
- 36) J. Plessel, M. M. Abd-Elmeguid, J. P. Sanchez, G. Knebel, C. Geibel, O. Trovarelli, and F. Steglich: *Phys. Rev. B* **67** (2003) 180403(R).
- 37) J. Custers, P. Gegenwart, H. Wilhelm, K. Neumaier, Y. Tokiwa, O. Trovarelli, F. Steglich, C. Pépin, and P. Coleman: *Nature* **424** (2003) 524.
- 38) S. Kimura, J. Sichelschmidt, J. Ferstl, C. Krellner, C. Geibel, and F. Steglich: *Phys. Rev. B* **74** (2006) 132408.
- 39) S. Paschen, T. Lühmann, S. Wirth, P. Gegenwart, O. Trovarelli, C. Geibel, F. Steglich, P. Coleman, and Q. Si: *Nature* **432** (2004) 881.
- 40) J. Sichelschmidt, J. Wykhoff, H.-A. Krug von Nidda, J. Ferstl, C. Geibel, and F. Steglich: *J. Phys.: Condens. Matter* **19** (2007) 116204.
- 41) Y. Tokiwa, P. Gegenwart, T. Radu, G. Sparn, C. Geibel, and F. Steglich: *Phys. Rev. Lett.* **94** (2005) 226402.
- 42) P. Gegenwart, T. Westerkamp, C. Krellner, Y. Tokiwa, S. Paschen, C. Geibel, F. Steglich, E. Abrahams, and Q. Si: *Science* **315** (2007) 969.
- 43) A. J. Millis, A. J. Schofield, G. G. Lonzarich, and S. A. Grigera: *Phys. Rev. Lett.* **88** (2002) 217204.
- 44) For a review, K. Miyake: *J. Phys.: Condens. Matter* **19** (2007) 125201.
- 45) A. T. Holmes, D. Jaccard, and K. Miyake: *Phys. Rev. B* **69** (2004) 024508.
- 46) P. Coleman, C. Pépin, Q. Si, and R. Ramazashvili: *J. Phys.: Condens. Matter* **13** (2001) R723.
- 47) M. R. Norman: *Phys. Rev. B* **71** (2005) 220405(R).
- 48) M. J. Besnus, J. P. Kappler, P. Lehman, and A. Meyer: *Solid State Commun.* **55** (1985) 779.
- 49) J. D. Thompson, J. O. Willis, C. Godard, D. E. MacLaughlin, and L. C. Gupta: *Solid State Commun.* **56** (1985) 169.
- 50) L. P. Regnault, W. A. C. Erkelens, and J. Rossat-Mignod, P. Lejay, and J. Flouquet: *Phys. Rev. B* **38** (1988) 4481.
- 51) H. Kadowaki, M. Sato, and S. Kawarazaki: *Phys. Rev. Lett.* **92** (2004) 097204.
- 52) H. Haen, J. P. Kappler, F. Lapiere, P. Lehman, P. Lejay, J. Flouquet, and A. Meyer: *J. Phys. C* **8** (1988) 757.
- 53) A. Amato, R. Feyerherm, F. N. Gygax, A. Schenck, J. Flouquet, and P. Lejay: *Phys. Rev. B* **50** (1994) R619.
- 54) J. Yoshida, S. Abe, D. Takahashi, Y. Segawa, Y. Komai, H. Tsujii, K. Matsumoto, H. Suzuki, and Y. Ōnuki: *Phys. Rev. Lett.* **101** (2008) 256402.
- 55) R. T. Macaluso, S. Nakatsuji, E. L. Thomas, Y. Machida, Y. Maeno, Z. Fisk, and J. Y. Chan: *Chem. Mater.* **19** (2007) 1918.
- 56) K. Kuga, Y. Karaki, Y. Matsumoto, Y. Machida, and S. Nakatsuji: *Phys. Rev. Lett.* **101** (2008) 137004.
- 57) Q. Si, S. Rabello, K. Ingersent, and J. L. Smith: *Nature* **413** (2001) 804.
- 58) H. Watanabe and M. Ogata: *Phys. Rev. Lett.* **99** (2007) 136401.
- 59) J. W. Clark, V. A. Khodel, and M. V. Zverev: *Phys. Rev. B* **71** (2005) 012401.
- 60) Q. Si: *Physica B* **378-380** (2006) 23.
- 61) A. Schröder, G. Aeppli, R. Coldea, M. Adams, O. Stockert, H. v. Löhneysen, E. Bucher, R. Ramazashvili, and P. Coleman: *Nature* **407** (2000) 351.
- 62) H. Bartolf, C. Pfleiderer, O. Stockert, M. Vojta, and H. v. Löhneysen: *Physica B* **359-361** (2005) 86.
- 63) R. E. Walstedt, H. Kojima, N. Butch, and N. Bernhoeft: *Phys. Rev. Lett.* **90** (2003) 067601.
- 64) P. Carretta, M. Giovannini, M. Horvatić, N. Papinutto, and A. Rigamonti: *Phys. Rev. B* **68** (2003) 220404(R).
- 65) O. Stockert, M. Enderle, and H. v. Löhneysen: *Phys. Rev. Lett.* **99** (2007) 237203.
- 66) I. M. Lifshitz: *Sov. Phys. JETP* **11** (1960) 1130 [Zh. Eksp. Teor. Fiz. **38** (1960) 1569].
- 67) Y. Yamaji, T. Misawa, and M. Imada: *J. Phys. Soc. Jpn.* **75** (2006) 094719.
- 68) Y. Yamaji, T. Misawa, and M. Imada: *J. Phys. Soc. Jpn.* **76** (2007) 063702.
- 69) T. Misawa, Y. Yamaji, and M. Imada: *J. Phys. Soc. Jpn.* **75** (2006) 083705.
- 70) T. Misawa and M. Imada: *Phys. Rev. B* **75** (2007) 115121.
- 71) M. Hatatani, O. Narikiyo, and K. Miyake: *J. Phys. Soc. Jpn* **67** (1998) 4002.
- 72) K. Umeo, H. Kadowaki, and T. Takabatake: *Phys. Rev. B* **55** (1997) R692.

- 73) I. Fischer and A. Rosch: Phys. Rev. B **71** (2005) 184429.
- 74) E. H. Graf, D. M. Lee, and J. D. Reppy: Phys. Rev. Lett. **19** (1967) 417.
- 75) M. Blume, V. J. Emery, and R. B. Griffiths: Phys. Rev. A **4** (1971) 1071.
- 76) M. M. Parish, F. M. Marchetti, A. Lamacraft, and B. D. Simons: Nature Phys. **3** (2007) 124.